

# COLLECT, COMMIT, EXPAND: EFFICIENT CPQR-BASED COLUMN SELECTION FOR EXTREMELY WIDE MATRICES

ROBIN ARMSTRONG\* AND ANIL DAMLE†

**Abstract.** Column-pivoted QR (CPQR) factorization is a computational primitive used in numerous applications that require selecting a small set of “representative” columns from a much larger matrix. These include applications in spectral clustering, model-order reduction, low-rank approximation, and computational quantum chemistry, where the matrix being factorized has a moderate number of rows but an extremely large number of columns. We describe a modification of the Golub-Businger algorithm which, for many matrices of this type, can perform CPQR-based column selection much more efficiently. This algorithm, which we call CCEQR, is based on a three-step “collect, commit, expand” strategy that limits the number of columns being manipulated, while also transferring more computational effort from level-2 BLAS to level-3. Unlike most CPQR algorithms that exploit level-3 BLAS, CCEQR is deterministic, and provably recovers a column permutation equivalent to the one computed by the Golub-Businger algorithm. Tests on spectral clustering and Wannier basis localization problems demonstrate that on appropriately structured problems, CCEQR can significantly outperform GEQP3.

**Key words.** column subset selection, QR factorization, column pivoting, spectral clustering, density functional theory

**MSC codes.** 65F25, 65F30, 62H30, 82-08

**1. Introduction.** The column subset selection problem (CSSP) appears in a remarkably wide range of applications. For example, certain nonlinear model order reduction techniques involve finding a small set of “informative” state components that capture the nonlinear term [7]. Some spectral clustering algorithms involve finding a small subset of data points containing one representative from each cluster [10]. And many low-rank approximation techniques require finding a small column subset whose span approximates the range of a larger matrix [30]. All of these problems can be treated as instances of CSSP.

Given a matrix  $\mathbf{A} \in \mathbb{C}^{m \times n}$  and an integer  $1 \leq k \leq \min\{m, n\}$ , CSSP entails finding  $k$  columns that are maximally large and linearly independent. This can be formalized as finding  $\mathbf{s} \in [n]^k$  that maximizes  $\sigma_{\min}(\mathbf{A}(:, \mathbf{s}))$ , which is an NP-hard combinatorial optimization problems [39]. In the communities of numerical linear algebra and theoretical computer science, significant effort has been devoted to finding efficient CSSP approximation algorithms over the course of several decades. Most of the resulting algorithms select columns using random sampling [12, 13, 14, 18, 28] or pivoted matrix factorizations [5, 6, 16, 19, 22, 24, 35], which themselves may be randomized [1, 26, 29, 32, 38]. The Golub-Businger algorithm for column-pivoted QR factorization [5] is a widely used column selection tool, owing to the fact that high-performance implementations exist and can be easily called from the standard libraries of most scientific computing languages. Although it has poor worst-case performance [22, 25], the empirical performance of this algorithm on realistic problems is usually quite strong [8].

A major difficulty in the Golub-Businger algorithm is that in a naïve implementation, Householder reflectors must be interwoven with column pivots. This precludes blocking the reflectors into compact forms that would allow a group of reflectors to be applied simultaneously with level-3 BLAS routines [3, 34], as opposed to sequen-

\*Cornell University, Center for Applied Mathematics, Ithaca, NY ([rja243@cornell.edu](mailto:rja243@cornell.edu)).

†Cornell University, Department of Computer Science, Ithaca, NY ([damle@cornell.edu](mailto:damle@cornell.edu)).

tially with much slower BLAS-2 operations. Like many authors before us, we will demonstrate a modification of the Golub-Businger algorithm that reduces BLAS-2 computation by allowing blocked application of Householder reflectors. Most prior work has achieved this by limiting BLAS-2 work to a small number of rows, either by transferring the entire pivot calculation onto a sketched matrix with shorter columns [26, 38], by reflecting single rows at a time to determine pivots while accumulating reflectors into compact WY blocks [31], or by generating reflectors and pivots in blocks using repeated sketches of the trailing submatrix [29]. Given that the Golub-Businger algorithm has  $\mathcal{O}(m^2n)$  complexity for an  $m \times n$  matrix, these techniques can dramatically speed up computation when  $m$  is moderate or large compared to  $n$ .

This paper, however, is concerned with situations where  $n$  vastly exceeds  $m$ . Several applications give rise to this sort of column subset selection problem. For example, spectral clustering [10] generates CSSP instances where each row corresponds to a cluster and each column corresponds to a single data point. Model order reduction [7] generates CSSP instances where each row corresponds to a coordinate of the reduced model and each column corresponds to a coordinate of the full model. In these examples and more, the number of columns may exceed the number of rows by several orders of magnitude. Unless the desired number of skeleton columns is much smaller than the number of rows, strategies based limiting BLAS-2 effort to a small number of rows do not effectively address the main bottleneck for these problems.

We will address this bottleneck using an algorithm that we call CCEQR (“Collect, Commit, Expand” QR). This algorithm repeatedly “collects” a set of heuristically good pivot candidates, “commits” a provably good subset of the candidates into the pivot sequence, and then “expands” the candidate search to a wider range of columns. Unlike column selection strategies for wide matrices that use parallelization [4, 11] or random sampling [12, 13, 14, 18, 28], CCEQR is deterministic, and provably selects the same column subset as the Golub-Businger algorithm (cf. [Theorem 3.2](#)). In terms of efficiency, the major advantages of CCEQR are that (1) Householder reflectors are only applied with BLAS-2 during the “commit” step, where they are limited to the small set of candidate columns, and (2) Householder reflectors in the “expand” step (applied with BLAS-3) are only applied to a small subset of “tracked” columns. We explain the details of this algorithm in [section 3](#).

In [section 4](#) we will show that for an appropriately structured problem, CCEQR can perform as much as an order of magnitude faster than the standard implementation of the Golub-Businger algorithm in LAPACK. By an “appropriately structured problem,” we mean two things. First, we are referring to problems where the relevant information to compute is the column permutation, rather than the full column-pivoted QR factorization. This includes the aforementioned problems in model order reduction [7], spectral clustering [10], and low-rank approximation [30], in addition to many others. Although CCEQR can be easily modified to compute a full CPQR factorization  $\mathbf{A}\mathbf{\Pi} = \mathbf{Q}\mathbf{R}$ , much of its efficiency derives from the fact that the main algorithm computes only  $\mathbf{Q}$ ,  $\mathbf{\Pi}$ , and a few columns of  $\mathbf{R}$ .

Second, matrices that are “appropriately structured” for CCEQR have the property that their column norm distribution is mostly concentrated on a small subset of column indices. This assumption is both reasonable and interpretable in many application areas. For instance, in spectral clustering [10], column norms in the relevant matrix are determined by the likelihoods of the corresponding data points under various clusters [33]. For these problems, CCEQR will perform well when a large number of data points are far from the center of any cluster. Density functional theory generates a column subset selection problem where column norms in the relevant matrix

are directly related to electron densities over a discretized spatial grid [9, 27]. These norms will decay rapidly under mild physical assumptions about the chemical system [2]. In section 4, we will empirically demonstrate how variations in problem structure impact the performance of CCEQR. In the worst cases, the runtime of CCEQR will still be comparable to (albeit slower than) the LAPACK implementation of the Golub-Businger algorithm.

**1.1. Code Availability.** A reference implementation of CCEQR in Julia is available at <https://github.com/robin-armstrong/CCEQR.jl>. A repository of Julia code to reproduce the numerical experiments in this paper can found at <https://github.com/robin-armstrong/cceqr-experiments>.

**1.2. Notation.** Matrices will be denoted with bold capital letters, vectors with bold lowercase letters, and all other objects with un-bolded letters. We use MATLAB notation to slice vectors and matrices by row or column. Thus, if  $\mathbf{x}$  is a vector, then  $\mathbf{x}(j)$  is its  $j^{\text{th}}$  entry. If  $\mathbf{A}$  is a matrix, then  $\mathbf{A}(i, :)$  denotes its  $i^{\text{th}}$  row,  $\mathbf{A}(:, j)$  its  $j^{\text{th}}$  column, and  $\mathbf{A}(i, j)$  its  $(i, j)$  element. When  $\mathbf{j} = [j_1, \dots, j_r]$  is a vector of column indices, we will write  $\mathbf{x}(\mathbf{j})$  to denote the vector  $[\mathbf{x}(j_1), \dots, \mathbf{x}(j_r)]$ ,  $\mathbf{A}(:, \mathbf{j})$  to denote the matrix  $[\mathbf{A}(:, j_1) \cdots \mathbf{A}(:, j_r)]$ , and similar notation applies to rows. The symbol  $[n]$  represents the set  $\{1, 2, \dots, n\}$ , and when  $p \leq q$  are integers, the symbol  $p:q$  represents the vector  $[p, p+1, \dots, q-1, q]$ .

Indexed matrix products will be ordered from left to right. Thus, if  $\mathbf{A}_1, \dots, \mathbf{A}_k$  are matrices of conformal dimensions, then  $\prod_{i=1}^k \mathbf{A}_i := \mathbf{A}_1 \mathbf{A}_2 \dots \mathbf{A}_k$ .

**2. Background.** Here we will review the necessary background material for this paper, including column-pivoted and rank-revealing QR factorizations, the Golub-Businger algorithm, blocking techniques for Householder reflectors, and accelerated column selection strategies based on randomization and parallelization.

**2.1. CPQR Factorizations.** Given  $\mathbf{A} \in \mathbb{C}^{m \times n}$  and  $k \in \{1, \dots, \min\{m, n\}\}$ , a column-pivoted QR (CPQR) factorization of  $\mathbf{A}$  has the form

$$\mathbf{Q}^* \mathbf{A} \mathbf{\Pi} = \begin{bmatrix} \mathbf{R}_{11} & \mathbf{R}_{12} \\ \mathbf{0} & \mathbf{R}_{22} \end{bmatrix}$$

where  $\mathbf{Q} \in \mathbb{C}^{m \times m}$  is unitary,  $\mathbf{\Pi} \in \{0, 1\}^{n \times n}$  is a permutation, and  $\mathbf{R}_{11} \in \mathbb{C}^{k \times k}$  is upper-triangular. The first  $k$  columns of  $\mathbf{\Pi}$  define an index vector  $\mathbf{s}$  such that  $\mathbf{A} \mathbf{\Pi}(:, 1:k) = \mathbf{A}(:, \mathbf{s})$ . CPQR algorithms construct  $\mathbf{\Pi}$  in order to satisfy two basic conditions, which can be informally stated as (1) the columns of  $\mathbf{A}(:, \mathbf{s})$  are large and well-conditioned, and (2) range  $\mathbf{A}(:, \mathbf{s})$  is a low-dimensional approximation of range  $\mathbf{A}$ .

More formally, CPQR algorithms choose  $\mathbf{\Pi}$  such that

$$(2.1) \quad \sigma_{\min}(\mathbf{A}(:, \mathbf{s})) \geq \frac{\sigma_k(\mathbf{A})}{q(n, k)} \quad \text{and} \quad \|\mathbf{A} - \mathbf{A}(:, \mathbf{s}) \mathbf{A}(:, \mathbf{s})^\dagger \mathbf{A}\|_2 \leq q(n, k) \sigma_{k+1}(\mathbf{A}),$$

where  $q$  is a function determined by the algorithm’s design that bounds the suboptimality of the factorization<sup>1</sup>. If  $q$  is bounded by a low-degree bivariate polynomial then the algorithm is said to compute a “rank-revealing” QR factorization [6, 8, 22, 24]. Although they have a strong near-optimality guarantee, rank-revealing QR factorization algorithms are complex to implement and, crucially, are not implemented

<sup>1</sup>This function bounds suboptimality because  $\sigma_{\min}(\mathbf{A}(:, \mathbf{j})) \leq \sigma_k(\mathbf{A})$  for any  $\mathbf{j} \in [n]^k$  (a consequence of singular value interlacing), and  $\|\mathbf{A} - \mathbf{A}(:, \mathbf{j}) \mathbf{B}\|_2 \geq \sigma_{k+1}(\mathbf{A})$  for any  $(\mathbf{j}, \mathbf{B}) \in [n]^k \times \mathbb{C}^{k \times n}$  (a consequence of the Eckart-Young theorem).

in LAPACK. This paper focuses on the much more commonly used Golub-Businger algorithm [5], implemented in LAPACK as GEQP3.

**2.2. The Golub-Businger Algorithm.** Rather than maximizing  $\sigma_{\min}(\mathbf{A}(:, \mathbf{s}))$  over  $\mathbf{s} \in [n]^k$ , the Golub-Businger algorithm [5] constructs a column permutation which solves a related but more computationally tractable problem: that of reducing a matrix to  $k$ -Golub-Businger form.

DEFINITION 2.1. *Let  $\mathbf{R} \in \mathbb{C}^{m \times n}$  and  $k \leq \min\{m, n\}$ . We say that  $\mathbf{R}$  has  $k$ -Golub-Businger form, or GB( $k$ ) form, if its first  $k$  columns are upper-triangular and satisfy*

$$(2.2) \quad |\mathbf{R}(i, i)| = \max_{i \leq j \leq n} \|\mathbf{R}(i : m, j)\|_2$$

for  $1 \leq i \leq k$ . We observe the convention that all matrices are in GB(0) form.

The first  $k$  columns of a GB( $k$ )-form matrix represent a “greedily optimal” column subset for large norms and good conditioning, in the following sense: for  $1 \leq i \leq k$ , the  $i^{\text{th}}$  column has maximal norm in the subspace orthogonal to the previous  $i - 1$ . Given  $\mathbf{A} \in \mathbb{C}^{m \times n}$ , the Golub-Businger algorithm computes a unitary  $\mathbf{Q}$  and a permutation  $\mathbf{\Pi}$  such that  $\mathbf{R} := \mathbf{Q}^* \mathbf{A} \mathbf{\Pi}$  has GB( $k$ ) form. This is accomplished by setting  $\mathbf{R} \leftarrow \mathbf{A}$ ,  $\mathbf{Q} \leftarrow \mathbf{I}_{m \times m}$ ,  $\mathbf{\Pi} \leftarrow \mathbf{I}_{n \times n}$ , and then repeating the following actions for  $i = 1, \dots, k$ :

1. Locate the column with largest norm orthogonal to range  $\mathbf{R}(i : m, 1 : (i - 1))$ . Due to the upper-triangular structure in  $\mathbf{R}(i : m, 1 : (i - 1))$ , this corresponds to finding  $j_{\max} \in \arg \max_{i \leq j \leq n} \|\mathbf{R}(i : m, j)\|_2$ .
2. Move this column to index  $i$ , and record this permutation by modifying  $\mathbf{\Pi}$ .
3. Apply a rotation that creates zeros in the  $((i + 1) : m, i)$  block of  $\mathbf{R}$ , and record this rotation by modifying  $\mathbf{Q}$ .

The LAPACK routine GEQP3 implements this algorithm with  $k = \min\{m, n\}$ .

We summarize the Golub-Businger algorithm in [Algorithm 2.1](#). The efficiency and numerical stability of this algorithm depends critically on the use of Householder reflections in lines (9) through (11), the details of which are discussed in [subsection 2.3](#). Fast implementations of this algorithm such as GEQP3 include several performance optimizations which the pseudocode in [Algorithm 2.1](#) does not capture. For example,  $\mathbf{Q}$  is represented in compressed form in terms of its Householder vectors,  $\mathbf{\Pi}$  is stored as a vector, and recursive update formulas are used to avoid recalculating column norms from scratch at line (5). See [20, sec 5.4.2] for details, and [15] for a discussion of numerical stability in the column-norm updates.

The Golub-Businger algorithm satisfies (2.1) with  $q(n, k) = 2^k \sqrt{n - k}$  [22], though the actual performance of this algorithm is usually much better than the exponential factor in  $k$  would suggest [8]. This exponential factor reflects the fact that for certain pathological matrices, notably the  $n \times n$  Kahan matrix with  $k = n - 1$ , the Golub-Businger algorithm selects a column subset with highly suboptimal conditioning [25]. Such matrices are almost never encountered in real-world applications.

**2.3. Householder Reflections and Compact WY Form.** The unitary matrix  $\mathbf{Q} \in \mathbb{C}^{m \times m}$  produced by [Algorithm 2.1](#) has the form  $\mathbf{Q} = \mathbf{Q}_1 \mathbf{Q}_2 \dots \mathbf{Q}_k$ , where  $\mathbf{Q}_i \in \mathbb{C}^{m \times m}$  is a unitary matrix such that  $\mathbf{Q}_i^*$  creates zeros in the  $((i + 1) : m, i)$  block of  $\mathbf{R}$ . Efficient implementations of QR factorization algorithms do not form  $\mathbf{Q}_i$  explicitly, but instead represent it in terms of a  $\mathbf{v}_i \in \mathbb{C}^m$  and  $\tau_i \geq 0$  such that  $\mathbf{Q}_i = \mathbf{I} - \tau_i \mathbf{v}_i \mathbf{v}_i^*$ . In [Algorithm 2.1](#),  $\mathbf{v}_i$  and  $\tau_i$  are computed at line (9), where  $\mathbf{v}, \tau \leftarrow \text{householder}(\mathbf{x}, i)$

---

**Algorithm 2.1** GOLUB-BUSINGER ALGORITHM
 

---

1: **inputs:**  $\mathbf{A} \in \mathbb{C}^{m \times n}$  (input matrix),  $k \leq \min\{m, n\}$  (desired skeleton size).  
 2: **outputs:**  $\mathbf{Q}, \mathbf{R}, \mathbf{\Pi}$  (factors of a CPQR factorization with  $\mathbf{R}$  in GB( $k$ ) form).

3: initialize  $\mathbf{Q} \leftarrow \mathbf{I}_{m \times m}$ ,  $\mathbf{R} \leftarrow \mathbf{A}$ , and  $\mathbf{\Pi} \leftarrow \mathbf{I}_{n \times n}$ .  
 4: **for**  $i = 1, 2, \dots, k$  **do**  
 5:   find  $j_{\max} \in \arg \max_{j \geq i} \|\mathbf{R}(i:m, j)\|_2$ .  
 6:   swap columns  $i$  and  $j_{\max}$  in  $\mathbf{R}$ .  
 7:   swap columns  $i$  and  $j_{\max}$  in  $\mathbf{\Pi}$ .  
 8:   **if**  $i < k$  **then**  
 9:     compute  $\mathbf{v}_i, \tau_i \leftarrow \text{householder}(\mathbf{R}(:, i), i)$ .  
 10:    update  $\mathbf{R} \leftarrow \mathbf{R} - \tau_i \mathbf{v}_i (\mathbf{v}_i^* \mathbf{R})$ .  
 11:    update  $\mathbf{Q} \leftarrow \mathbf{Q} - \tau_i (\mathbf{Q} \mathbf{v}_i) \mathbf{v}_i^*$ .  
 12:    **end if**  
 13: **end for**  
 14: **return**  $\mathbf{Q}, \mathbf{R}, \mathbf{\Pi}$ .

---

produces a “Householder vector”  $\mathbf{v} \in \mathbb{C}^m$  and a “Householder scalar”  $\tau \geq 0$  such that

$$\begin{aligned} \mathbf{v}(1) &= \dots = \mathbf{v}(i-1) = 0 \\ \mathbf{v}(i) &= 1 \\ (\mathbf{I} - \tau \mathbf{v} \mathbf{v}^*) (\mathbf{I} - \tau \mathbf{v} \mathbf{v}^*) &= \mathbf{I} \\ (\mathbf{I} - \tau \mathbf{v} \mathbf{v}^*) \mathbf{x} &= [\mathbf{x}(1), \dots, \mathbf{x}(i-1), \mu, 0, \dots, 0], \quad |\mu| = \pm \|\mathbf{x}(i:m)\|_2. \end{aligned}$$

The matrix  $\mathbf{I} - \tau \mathbf{v} \mathbf{v}^*$  is called a “Householder reflection” [20, sec. 5.1.2].

Because  $\mathbf{Q}$  is implicitly represented through  $\mathbf{v}_1, \dots, \mathbf{v}_k$  and  $\tau_1, \dots, \tau_k$ , left-multiplying a matrix  $\mathbf{X}$  by  $\mathbf{Q}$  or  $\mathbf{Q}^*$  involves  $k$  updates of the form  $\mathbf{X} \leftarrow \mathbf{X} - \tau_i \mathbf{v}_i (\mathbf{v}_i^* \mathbf{X})$ , with  $\mathbf{v}_i^* \mathbf{X}$  computed by level-2 BLAS operations. Vectorization and multithreading considerations mean that a single  $(k \times m) \cdot (m \times n)$  product with level-3 BLAS is significantly faster than  $k$  sequential  $(1 \times m) \cdot (m \times n)$  products with level-2 BLAS [20, sec. 1.5]. For this reason, it is advantageous to define  $\mathbf{V} = [\mathbf{v}_1 \dots \mathbf{v}_k] \in \mathbb{C}^{m \times k}$  and to seek a  $\mathbf{T} \in \mathbb{C}^{k \times k}$  such that

$$(2.3) \quad \mathbf{Q} = \mathbf{I} - \mathbf{V} \mathbf{T} \mathbf{V}^*,$$

so that  $\mathbf{Q}$  can be efficiently applied using  $\mathbf{Q} \mathbf{X} = \mathbf{X} - \mathbf{V} \mathbf{T} (\mathbf{V}^* \mathbf{X})$ , with  $\mathbf{V}^* \mathbf{X}$  evaluated using level-3 BLAS routines.

If  $\mathbf{V}$  is lower-triangular with unit diagonal and  $\mathbf{T}$  is upper-triangular, then we say that (2.3) constitutes a *compact WY form* of  $\mathbf{Q}$  [34]. Representing  $\mathbf{Q}$  in compact WY form is straightforward when  $(\mathbf{v}_1, \tau_1), \dots, (\mathbf{v}_k, \tau_k)$  are generated by Algorithm 2.1, for two reasons. First, the upper-triangular structure of  $\mathbf{R}$  already ensures that  $\mathbf{V} = [\mathbf{v}_1 \dots \mathbf{v}_k]$  is lower-triangular with unit diagonal. Second, regardless of the structure  $\mathbf{V}$ , an upper-triangular  $\mathbf{T}$  satisfying (2.3) always exists and can be easily generated using an algorithm developed by Schreiber and Van Loan [34].

**2.4. Accelerated CPQR Algorithms.** When the dimensions of  $\mathbf{A}$  are extremely large, Algorithm 2.1 suffers a computational bottleneck that results from sequential applications of Householder reflections using level-2 BLAS operations. For non-pivoted QR factorizations, it is standard practice to limit level-2 BLAS work by

manipulating columns in blocks, where each block yields a set of Householder vectors that are accumulated into compact WY form for later application to the rest of the matrix using level-3 BLAS [20, sec 5.2.3]. In Algorithm 2.1, however, Householder reflectors are determined on the basis of a column swap which requires all previous reflections to be applied to the matrix *before* a compact WY representation can be formed. In this setting, limiting the amount of work performed at level-2 BLAS is more difficult.

This paper describes a modification of Algorithm 2.1 that addresses this bottleneck for matrices with certain structure, but we are by no means the first authors to tackle this problem. A large class of algorithms have been proposed that reduce the number of rows manipulated by level-2 BLAS, such as the following.

**Partial Householder reflections.** Selecting pivot columns in line (5) of Algorithm 2.1 requires knowledge of column norms in the  $(i:m, i:n)$  block of  $(\mathbf{I} - \tau_i \mathbf{v}_i \mathbf{v}_i^*) \mathbf{R}$  as computed in line (10), but it is well known that only the first row of this matrix is needed to determine these norms [20, sec 5.4.2]. Quianta-Ortí, Sun, and Bishof [31] use this fact to limit level-2 BLAS work to a small number of rows. Their method is to select pivot columns in blocks where, at each step, a Householder reflection is applied “partially” to reveal the single row needed to update column norms. Meanwhile, reflections are accumulated into a compact WY form that allows the remaining rows to be updated with level-3 BLAS at the end of the block. This strategy is used in GEQP3, the LAPACK implementation of Algorithm 2.1.

**Sketching.** Many tasks in numerical linear algebra can be accelerated by first generating a random “sketching matrix”  $\mathbf{\Omega} \in \mathbb{R}^{m \times d}$ , with  $d \ll m$  [23]. If drawn from a suitable distribution,  $\mathbf{\Omega}$  induces a transform  $\mathbf{x} \mapsto \mathbf{\Omega}^* \mathbf{x}$  that randomly embeds vectors in a much lower dimensional space, while approximately preserving geometry in a sense made precise by the Johnson-Lindenstrauss lemma [36, Thm 1.6.1]. Duersch and Gu [17] used this fact to devise an “RCPQR” algorithm which selects pivot columns using a CPQR factorization of  $\mathbf{\Omega}^* \mathbf{A}$ , where the entries of  $\mathbf{\Omega}$  are i.i.d. standard Gaussians. This limits BLAS-2 computation to the much smaller number of rows in  $\mathbf{\Omega}^* \mathbf{A}$ , and once pivot columns are selected, the remaining transformations necessary to CPQR-factorize  $\mathbf{A}$  proceed with BLAS-3. A related class of “randomized interpolative decomposition” (RID) algorithms use sketching with non-Gaussian  $\mathbf{\Omega}$  to form a column-based low-rank approximation of  $\mathbf{A}$  [26, 38].

**Randomized blocking.** Because RCPQR selects at most  $r := \text{rank } \mathbf{\Omega}^* \mathbf{A}$  skeleton columns, the constraint  $r \leq \min\{d, n\}$  means that modifications are needed when a full set of  $\min\{m, n\}$  skeleton columns is desired. In this vein, Martinsson et al. [29] describe a variant of Algorithm 2.1 which selects a full skeleton set in blocks of  $b$ , where each block is selected by applying RCPQR with  $d = b$  to the trailing submatrix of  $\mathbf{R}$ . The Householder reflections generated for each block can be accumulated into compact WY form and applied to the rest of the matrix with BLAS-3.

**GKS and DEIM.** If only  $k \ll n$  skeleton columns are needed, the GKS [19] and DEIM [35] algorithms provide a means to select these columns by pivoting on a matrix of only  $k$  rows, corresponding to the leading  $k$  right singular vectors of  $\mathbf{A}$ . Computing these vectors is, in and of itself, a computationally intensive task. For this reason, randomized GKS [1] or randomized DEIM [32] algorithms that estimate the leading singular vectors with sketching may be preferable.

This paper is interested in matrices that have far more columns than rows, such that the techniques above do not address the main bottleneck. Matrices of this aspect ratio are amenable to a separate class of algorithms that leverage parallelization or randomization. These include the following.

**Global and local pivoting.** Bishof [4] describes two modifications of [Algorithm 2.1](#) that parallelize the column load across several processors, a “global” version and a “local” one. The “global” algorithm distributes column norm updates across different processors, which each send updated norms to a “lead” processor with authority to choose the next pivot. To avoid the bottleneck that results from each processor waiting for the lead’s decision, the “local” pivoting method equips each processor with an incremental condition number estimator that allows it to select pivot columns on its own. Both strategies employ row-restricted Householder reflections, as in [31], to allow norm updates and pivot selections to be performed more-or-less simultaneously.

**Tournament pivoting.** Demmel et al. [11] developed a parallelized CPQR factorization algorithm that selects pivots in blocks of  $b$ , while minimizing the communication cost associated with column movement for each block. This is accomplished in a multi-level “tournament,” where at the first level, each processor is assigned a small block of columns from which it selects  $b$  skeleton columns using a rank-revealing QR (RRQR) factorization. At the next level, each processor is assigned a combined block of  $2b$  skeleton columns which is again downsampled to  $b$  columns by an RRQR factorization. After  $\mathcal{O}(\log n)$  rounds of the tournament, a block of  $b$  columns has been selected; this is repeated until a full skeleton set is obtained.

**Random sampling.** While they are not CPQR algorithms *per se*, there is a large class of algorithms developed in theoretical computer science that choose column subsets by randomly sampling from an appropriate distribution. The first algorithms in this category sampled based on column norm alone [18], while later algorithms sampled based on subspace leverage scores [14, 28]. These methods require significant oversampling. A related class of “volume sampling” algorithms sample columns in batches that bias towards high linear independence [12, 13]. These do not require the same degree of oversampling, but the samples themselves are more expensive to generate.

These algorithms are effective at rapidly selecting columns from matrices with far more columns than rows. In [section 3](#), we will focus on accelerating the Golub-Businger algorithm ([Algorithm 2.1](#)) for matrices of this sort. [Algorithm 2.1](#) is distinguished from the techniques just described by the fact that its column choice satisfies a readily interpretable greedy ordering, namely, that of  $GB(k)$  form. In practice, this does not make [Algorithm 2.1](#) perform significantly better or worse than the other algorithms described here in the sense of optimizing the rank-revealing bound [\(2.1\)](#).

**3. The CCEQR Algorithm.** The main contribution of this paper is CCEQR (“Collect, Commit, Expand” QR), a modification of the Golub-Businger algorithm that enables highly efficient CPQR-based column selection. Like many such algorithms, CCEQR employs a blocked pivoting strategy that allows Householder reflections to be applied with level-3 BLAS. But when compared with other blocked pivoting strategies (cf. [subsection 2.4](#)), CCEQR differs in two important respects. First, existing blocked pivoting algorithms limit BLAS-2 work to a small number of rows using either randomized sketching [26, 29, 38] or row-restricted Householder reflections [31]. CCEQR, on the other hand, is designed for matrices that have a moderate number of rows and an extreme number of columns, such that reducing the number of rows being operated on would not address the main computational bottleneck. Second, unlike blocked pivoting methods that employ sketching, CCEQR is deterministic, and provably recovers a column permutation equivalent to the one computed by the Golub-Businger algorithm. By this, we mean that it always reduces its input matrix

to GB( $k$ ) form (cf. [Definition 2.1](#)).

CCEQR works in cycles, each of which pivots at least one column into the skeleton set. Each cycle starts with a permutation  $\mathbf{\Pi}$  and a unitary  $\mathbf{Q}$  such that  $\mathbf{Q}^* \mathbf{A} \mathbf{\Pi}$  has GB( $s$ ) form for some  $s \geq 0$ . The columns of  $\mathbf{A} \mathbf{\Pi}$  are partitioned into three contiguous blocks:

1. The leftmost block contains  $s$  “committed” skeleton columns. These will not be modified by the present cycle or by any future cycles.
2. The middle block contains “tracked” columns whose norms in the subspace orthogonal to  $\mathbf{A} \mathbf{\Pi}(:, 1:s)$  are monitored by the algorithm.
3. The rightmost block contains “untracked” columns, for which the only information known to CCEQR is the starting norm.

The objective of a given cycle is to modify  $\mathbf{\Pi}$  and  $\mathbf{Q}$  such that  $\mathbf{Q}^* \mathbf{A} \mathbf{\Pi}$  has GB( $s + c$ ) form for some  $c \geq 1$ . This is accomplished by a procedure which can be informally described as follows.

1. A “collect” step assembles a small set of candidate skeleton columns from the tracked set, and forms a CPQR factorization of the candidates.
2. A “commit” step uses the CPQR factors to identify  $c$  columns that can be safely added to the skeleton, and modifies  $\mathbf{\Pi}$  and  $\mathbf{Q}$  accordingly. If this action brings the skeleton to size  $k$ , then the algorithm terminates.
3. Otherwise, an “expand” step moves a portion of the untracked columns into the tracked set, adding new candidates to be collected at the next cycle.

After at most  $k$  cycles,  $\mathbf{Q}^* \mathbf{A} \mathbf{\Pi}$  will acquire GB( $k$ ) form. This cycle is represented schematically in [Figure 3.1](#).

Two major factors make this an efficient procedure for column selection. First, BLAS-2 Householder reflections are only used during the CPQR factorization in the “collect” step, during which they are only applied to small minority of columns (i.e., the candidate set). Second, and more significantly, Householder reflections in the “commit” and “expand” steps (performed with BLAS-3) are applied only to the set of tracked columns. This can greatly improve runtime, because if the parameters of CCEQR are properly tuned (cf. [section 4](#)), then the tracked set often represents a very small proportion of the entire matrix.

**3.1. Preliminaries.** At the outset of each cycle, CCEQR has computed a unitary  $\mathbf{Q} \in \mathbb{C}^{m \times m}$  and a permutation  $\mathbf{\Pi} \in \{0, 1\}^{n \times n}$  such that  $\mathbf{Q}^* \mathbf{A} \mathbf{\Pi}$  has GB( $s$ ) form for some  $s \geq 0$ , starting with  $\mathbf{Q} = \mathbf{I}_{m \times m}$ ,  $\mathbf{\Pi} = \mathbf{I}_{n \times n}$ , and  $s = 0$  at the first cycle. CCEQR applies column permutations globally, but for efficiency, rotations are applied only to the tracked set. Thus, CCEQR does not have explicitly compute  $\mathbf{Q}^* \mathbf{A} \mathbf{\Pi}$ , but instead computes

$$\mathbf{R} := \begin{bmatrix} \mathbf{R}_1 & \mathbf{R}_2 & \mathbf{X} \\ s & t & n - s - t \end{bmatrix}$$

where  $\mathbf{R}_1$  is an upper-triangular matrix corresponding to  $s$  “committed” skeleton columns,  $\mathbf{R}_2$  contains  $t$  “tracked” columns, and the remaining “untracked” columns make up  $\mathbf{X}$ . We have

$$[\mathbf{R}_1 \quad \mathbf{R}_2] = \mathbf{Q}^* \mathbf{A} \mathbf{\Pi}(:, 1:(s+t)) \quad \text{and} \quad \mathbf{X} = \mathbf{A} \mathbf{\Pi}(:, (s+t+1):n).$$



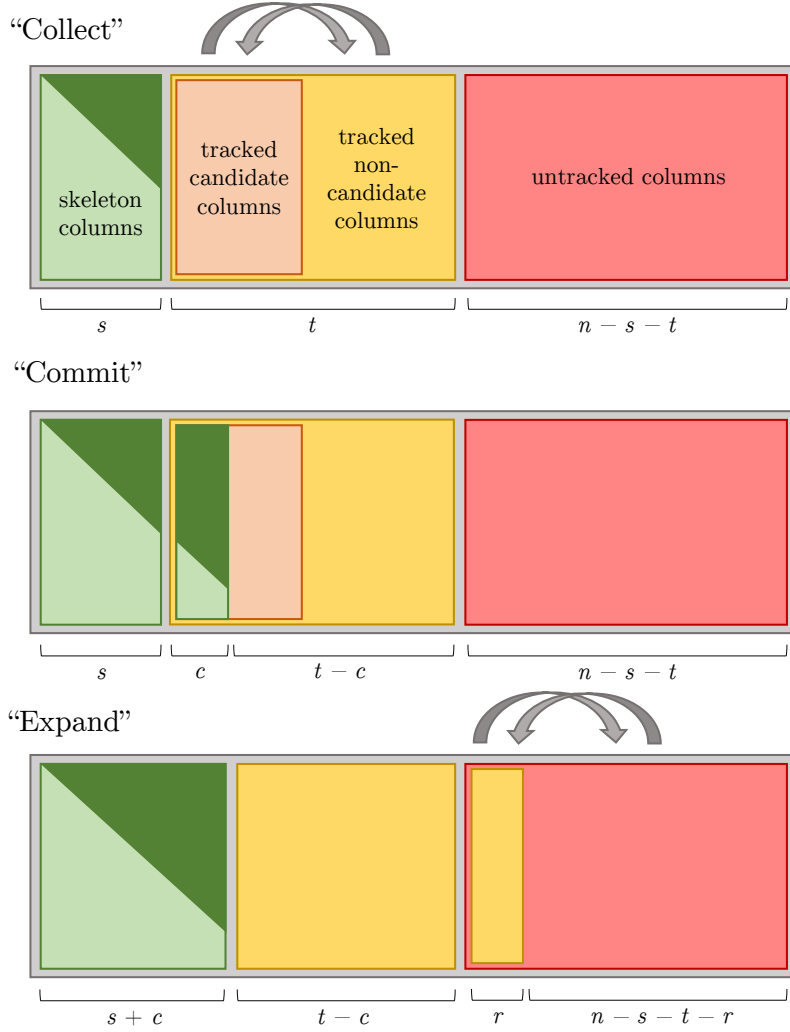


Fig. 3.1: A schematic representation of CCEQR. In the “collect” stage, a set of candidate skeleton columns are selected from the tracked set. The “commit” stage chooses a subset of these candidates to bring into the skeleton. The “expand” stage brings new columns into the tracked set.

CCEQR maintains a vector  $\gamma$  that records the *residual* norms of tracked columns, and the *overall* norms of untracked columns:

$$\gamma(j) = \begin{cases} \|\text{proj}_{(\text{range } \mathbf{A}\Pi(:,1:s))^\perp} \mathbf{A}\Pi(:,j)\|_2^2 & j \leq s + t \\ \|\mathbf{A}\Pi(:,j)\|_2^2 & j > s + t \end{cases}$$

The partition into committed, tracked, and untracked columns is maintained such that at the beginning of each cycle,

$$(3.1) \quad \max_{s < j \leq s+t} \gamma(j) \geq \max_{s+t < j} \gamma(j),$$

a relation which will ensure that each cycle of CCEQR adds at least one new skeleton column. Equation (3.1) holds automatically for the first cycle, which is initialized with  $s = 0$  and  $t = n$  (following the convention that  $|\mathbf{R}(0, 0)| = \infty$ ).

CCEQR also maintains a lower-triangular  $\mathbf{V}$  and upper-triangular  $\mathbf{T}$  providing a compact WY representation of  $\mathbf{Q}$ . These matrices are padded with zeros so that  $\mathbf{V} \in \mathbb{C}^{m \times k}$  and  $\mathbf{T} \in \mathbb{C}^{k \times k}$ , and the first cycle initializes with  $\mathbf{V} = \mathbf{0}_{m \times k}$ ,  $\mathbf{T} = \mathbf{0}_{k \times k}$ . Lastly,  $\mathbf{\Pi}$  is represented via a permutation vector  $\mathbf{p} \in [n]^n$  such that  $\mathbf{A}\mathbf{\Pi} = \mathbf{A}(:, \mathbf{p})$ ; this vector is modified by each cycle.

Algorithm 3.1 summarizes, in pseudocode, the steps taken to initialize the first cycle of CCEQR. Note that  $\mu$  stores the value of  $\max_{s+t < j} \gamma(j)$ .

---

**Algorithm 3.1** CCEQR: SUBROUTINE “INITIALIZE”

---

- 1: **inputs:**  $\mathbf{A}$ ,  $k$ .
  
  - 2:  $\mathbf{p} \leftarrow [1, 2, \dots, n]$ ,  $\mathbf{R} \leftarrow \mathbf{A}$ ,  $\mathbf{V} \leftarrow \mathbf{0}_{n \times k}$ , and  $\mathbf{T} \leftarrow \mathbf{0}_{k \times k}$ .
  - 3:  $s \leftarrow 0$ ,  $t \leftarrow n$ ,  $\mu \leftarrow 0$ .
  
  - 4: **for**  $j = 1, \dots, n$  **do**
  - 5:    $\gamma(j) \leftarrow \|\mathbf{R}(:, j)\|_2^2$ .
  - 6: **end for**
  
  - 7: **return**  $s, t, \mu, \gamma, \mathbf{p}, \mathbf{V}, \mathbf{T}, \mathbf{R}$ .
- 

**3.2. “Collect” Step.** This begins by forming a block of  $b$  “candidate” skeleton columns from the tracked set, where  $b = 1 + \lfloor \rho(t - 1) \rfloor$  and  $\rho \in (0, 1)$  is a fixed parameter set by the user<sup>2</sup>. Typically we use  $\rho \ll 1$  so that  $b \ll t$ . For the first cycle of CCEQR, which initializes with  $t = n$ , we follow this by setting  $t \leftarrow b + 1$ .

The candidate block consists of the tracked columns with largest residual norm, i.e., column indices

$$s + \boldsymbol{\sigma}(1:b) := [s + \boldsymbol{\sigma}(1), \dots, s + \boldsymbol{\sigma}(b)]$$

where  $\boldsymbol{\sigma}$  is a permutation vector that sorts  $\gamma((s + 1):(s + t))$  in descending order. After forming the candidate block, we must gather information that will be necessary for deciding which columns can be safely added to the skeleton in the “commit” step. To that end we record<sup>3</sup>

$$\delta := \max\{\gamma(j) : j \text{ is a non-candidate index in } [s + 1, s + t]\},$$

and we form a CPQR factorization of the candidate columns’ residuals:

$$(3.2) \quad \begin{aligned} \mathbf{B} &\leftarrow \mathbf{R}((s + 1):m, s + \boldsymbol{\sigma}(1:b)) \\ \hat{\mathbf{p}}, \hat{\boldsymbol{\tau}}, \hat{\mathbf{V}}, \hat{\mathbf{R}} &\leftarrow \text{GEQP3}(\mathbf{B}), \end{aligned}$$

---

<sup>2</sup>We define  $b$  in this way so that  $1 \leq b < t$  whenever  $t > 1$ , and otherwise  $b = t = 1$ .

<sup>3</sup>If all indices in  $[s + 1, s + t]$  are candidates, which occurs only if  $b = t = 1$ , then  $\delta := 0$ .

where  $\mathbf{b}$  is a permutation of  $1:b$ ,  $\widehat{\boldsymbol{\tau}} \in \mathbb{R}^d$  and  $\widehat{\mathbf{V}} \in \mathbb{C}^{(n-s) \times d}$  are Householder scalars and vectors (with  $d = \min\{m-s, b\}$ ), and  $\widehat{\mathbf{R}}$  is the resulting R-factor. To finish the “collect” step, we permute the candidate columns to indices  $(s+1):(s+b)$  of  $\mathbf{R}$  and reorder them according to  $\widehat{\mathbf{p}}$ . We also permute  $\boldsymbol{\gamma}$  and  $\boldsymbol{\gamma}$  for consistency. Because all column permutations up to this point have taken place within tracked set, equation (3.1) is still in force when the “collect” step terminates.

Algorithm 3.2 summarizes the “collect” step in pseudocode, where

$$\widehat{\mathbf{X}} \leftarrow \text{PermuteColumns}(\mathbf{X}, \mathbf{y}, \mathbf{z}, \mathbf{w})$$

reorders the columns of  $\mathbf{X}$  such that  $\widehat{\mathbf{X}}(:, \mathbf{z}) = \mathbf{X}(:, \mathbf{y}(\mathbf{w}))$ . `PermuteEntries` reorders the entries of a vector in an identical fashion.

---

**Algorithm 3.2** CCEQR: SUBROUTINE “COLLECT”

---

- 1: **inputs:**  $\rho, s, t, \boldsymbol{\gamma}, \mathbf{p}, \mathbf{R}$ .
  - 2:  $b \leftarrow 1 + \lfloor \rho(t-1) \rfloor$ .
  - 3:  $\boldsymbol{\sigma} \leftarrow$  permutation of  $1:t$  that sorts  $\boldsymbol{\gamma}((s+1):(s+t))$  in decreasing order.
  - 4:  $\delta \leftarrow \boldsymbol{\gamma}(s + \boldsymbol{\sigma}(b+1))$  **if**  $b < t$ , **else** 0.
  - 5: **if** FIRST-CYCLE **then**  $t \leftarrow b$ .
  - 6:  $\widehat{\mathbf{p}}, \widehat{\boldsymbol{\tau}}, \widehat{\mathbf{V}}, \widehat{\mathbf{R}} \leftarrow \text{GEQP3}(\mathbf{R}((s+1):m, s + \boldsymbol{\sigma}(1:b)))$ .
  - 7:  $\mathbf{R} \leftarrow \text{PermuteColumns}(\mathbf{R}, s + \boldsymbol{\sigma}(1:b), (s+1):(s+b), \widehat{\mathbf{p}})$ .
  - 8:  $\boldsymbol{\gamma} \leftarrow \text{PermuteEntries}(\boldsymbol{\gamma}, s + \boldsymbol{\sigma}(1:b), (s+1):(s+b), \widehat{\mathbf{p}})$ .
  - 9:  $\mathbf{p} \leftarrow \text{PermuteEntries}(\mathbf{p}, s + \boldsymbol{\sigma}(1:b), (s+1):(s+b), \widehat{\mathbf{p}})$ .
  - 10: **return**  $\delta, \widehat{\boldsymbol{\tau}}, \widehat{\mathbf{V}}, \widehat{\mathbf{R}}$ .
- 

**3.3. “Commit” Step.** The goal in this step is to modify  $\mathbf{Q}$  and  $\boldsymbol{\Pi}$  based on information prepared during the “collect” step such that  $\mathbf{Q}^* \mathbf{A} \boldsymbol{\Pi}$  has GB( $s+c$ ) form for some  $c \geq 1$ . Following this, columns  $1:(s+c)$  will count as “committed” skeleton columns, in the sense that no future cycle will modify or reorder them. The appropriate changes to  $\mathbf{Q}$  and  $\boldsymbol{\Pi}$  are determined using Lemma 3.1.

LEMMA 3.1. *Let  $\delta, \widehat{\boldsymbol{\tau}}, \widehat{\mathbf{V}}, \widehat{\mathbf{R}}$  be the data returned by the “collect” step of CCEQR (Algorithm 3.2), and let  $\widehat{\boldsymbol{\Pi}}$  be the column permutation matrix applied in line (7) of that step. Let  $\mu = \max_{s+t < j} \|\mathbf{A} \boldsymbol{\Pi}(:, j)\|_2^2$ , and define*

$$(3.3) \quad c = \max\{i \geq 1 : |\widehat{\mathbf{R}}(i, i)|^2 \geq \delta \vee \mu\}.$$

Let  $\widehat{\mathbf{Q}}$  be the unitary matrix that applies the first  $c$  Householder reflections computed in the “collect” step to the bottom  $n-s$  rows, i.e.,

$$\widehat{\mathbf{Q}} = \begin{bmatrix} \mathbf{I}_{s \times s} & \mathbf{0}_{s \times (n-s)} \\ \mathbf{0}_{(n-s) \times s} & \prod_{i=1}^c (\mathbf{I} - \boldsymbol{\tau}(i) \widehat{\mathbf{V}}(:, i) \widehat{\mathbf{V}}(:, i)^*) \end{bmatrix}.$$

Then,  $(\mathbf{Q} \widehat{\mathbf{Q}})^* \mathbf{A} (\boldsymbol{\Pi} \widehat{\boldsymbol{\Pi}})$  has GB( $s+c$ ) form.

*Proof.* A detailed proof is given in Appendix A. A proof sketch is as follows: (3.1) guarantees that the maximum in (3.3) is over a nonempty set, so  $c \geq 1$  is well-defined. To bring  $\mathbf{R}$  to GB( $k$ ) form in the usual way, we would apply Algorithm 2.1 to  $\mathbf{B}_1 :=$

$\mathbf{R}((s+1):m, (s+1):n)$ . In the “collect” step, we have instead applied [Algorithm 2.1](#) to  $\mathbf{B}_2 := \mathbf{R}((s+1):m, (s+1):(s+b))$ . The resulting column permutation brings  $\mathbf{R}$  to  $\text{GB}(s+c_0)$  form, where  $c_0$  is the number of iterations before [Algorithm 2.1](#) applied to  $\mathbf{B}_1$  selects a different column than it would if applied to  $\mathbf{B}_2$ . This occurs when there is a non-candidate column whose residual norm (if included in pivoting) would be bigger than that of any of the candidates. Equation (3.3) causes CCEQR to only “commit” a pivot columns if its residual is greater than the *overall* norm of all non-candidates. Thus ensuring no unwanted columns are accepted.  $\square$

As noted in the statement of [Lemma 3.1](#), the permutation  $\mathbf{\Pi} \mapsto \mathbf{\Pi}\widehat{\mathbf{\Pi}}$  was already performed by the “collect” step at line (7). It remains to update  $\mathbf{Q} \mapsto \mathbf{Q}\widehat{\mathbf{Q}}$  by incorporating the first  $c$  Householder reflectors from the “collect” step into the compact WY form for  $\mathbf{Q}$ . To that end, the Schreiber-van Loan algorithm [34] is used to form an upper-triangular  $\widehat{\mathbf{T}} \in \mathbb{C}^{c \times c}$  such that

$$\prod_{i=1}^c (\mathbf{I} - \tau(i)\widehat{\mathbf{V}}(:,i)\widehat{\mathbf{V}}(:,i)^*) = \mathbf{I} - \widehat{\mathbf{V}}(:,1:c)\widehat{\mathbf{T}}\widehat{\mathbf{V}}(:,1:c)^*.$$

In preparation for residual column norm updates, this rotation is applied to the bottom  $n-s$  rows of the tracked set. We then update  $\mathbf{Q}$  by incorporating  $\widehat{\mathbf{T}}$  and  $\widehat{\mathbf{V}}(:,1:c)$  into the global compact WY factors  $\mathbf{T}$  and  $\mathbf{V}$ . Although we could incorporate each reflector serially using the Schreiber-Van Loan algorithm [34], we instead apply a block update to the WY factors using a small number of BLAS-3 operations. The details of this are explained in [Appendix B](#).

Residual column norms are now updated in the tracked set by computing

$$(3.4) \quad \gamma(j) \leftarrow \gamma(j) - \|\mathbf{R}((s+1):(s+c), j)\|_2^2$$

for  $j = s+c+1, \dots, s+t$ . Note that  $\|\mathbf{R}((s+1):(s+c), j)\|_2^2$  represents the portion of  $\mathbf{R}(:,j)$  spanned by the newly committed skeleton columns. We record these new commits by setting  $s \leftarrow s+c$  and  $t \leftarrow t-c$ . The numerical stability of the column-norm update in (3.4) could be improved using techniques from [15], though we do not do this here.

[Algorithm 3.3](#) summarizes the “commit” step. In this pseudocode, the function  $\mathbf{X} \leftarrow \text{CompactWY}(\mathbf{x}, \mathbf{Y})$  takes as input Householder scalars  $\mathbf{x}$  and reflectors  $\mathbf{Y}$ , and returns the upper-triangular  $\mathbf{X}$  needed to represent the corresponding unitary matrix in compact WY form. The function  $\widehat{\mathbf{S}} \leftarrow \text{ApplyQt}(\mathbf{S}, \mathbf{X}, \mathbf{Y}, \mathbf{i}, \mathbf{j})$  applies a compact WY-form rotation  $(\mathbf{I} - \mathbf{Y}\mathbf{X}\mathbf{Y}^*)^*$  to the  $(\mathbf{i}, \mathbf{j})$  block of  $\mathbf{S}$  using BLAS-3 routines<sup>4</sup>. Lastly, `UpdateWY` adds new Householder reflectors to  $\mathbf{Q}$  using formulas in [Appendix B](#).

**3.4. “Expand” Step.** This step executes if the “commit” step did not complete the skeleton (i.e.,  $s+c < k$ ) and there are still untracked columns (i.e.,  $s+t < n$ ). In this case, because the tracked columns were orthogonalized against new skeleton columns, it is possible that their residual norms have decreased leading to a violation of inequality (3.1). To ensure that the next cycle is able to commit at least 1 additional skeleton column, we must modify the partition into “tracked” and “untracked” columns such that (3.1) is restored.

To that end, the “expand” step assembles an index vector  $\mathbf{u}$  containing all untracked indices  $j$  such that  $\|\mathbf{A}\mathbf{\Pi}(:,j)\|_2^2 \geq \max_{s < j \leq s+t} \gamma(j)$ . These indices will be

<sup>4</sup>To fully take advantage of BLAS-3 alongside the triangular structures inherent to compact WY form, our implementation of this function is templated off of the LAPACK routine LARFB.

---

**Algorithm 3.3** CCEQR: SUBROUTINE “COMMIT”

---

1: **inputs:**  $\delta, \mu, s, t, \gamma, \hat{\tau}, \hat{\mathbf{V}}, \mathbf{T}, \mathbf{V}, \hat{\mathbf{R}}, \mathbf{R}$ .

2:  $c \leftarrow \max\{i \geq 1 : |\hat{\mathbf{R}}(i, i)|^2 \geq \delta \vee \mu\}$ .

3:  $\hat{\mathbf{T}} \leftarrow \text{CompactWY}(\hat{\tau}(1:c), \hat{\mathbf{V}}(:, 1:c))$ .

4:  $\mathbf{R} \leftarrow \text{ApplyQt}(\mathbf{R}, \hat{\mathbf{T}}, \hat{\mathbf{V}}(:, 1:c), (s+1):m, (s+1):(s+t))$ .

5:  $\mathbf{T}, \mathbf{V} \leftarrow \text{UpdateWY}(\mathbf{T}, \mathbf{V}, \hat{\mathbf{T}}, \hat{\mathbf{V}}(:, 1:c))$ .

5:  $M \leftarrow 0$ .

6: **for**  $j = (s+1):(s+t)$  **do**

7:    $\gamma(j) \leftarrow \gamma(j) - \|\mathbf{R}((s+1):(s+c), j)\|_2^2$ .

8:    $M \leftarrow \max(M, \gamma(j))$ .

9: **end for**

10:  $s \leftarrow s + c$ .

11:  $c \leftarrow c - t$ .

12: **return**  $M$ .

---

moved from untracked to tracked<sup>5</sup>. While assembling  $\mathbf{u}$ , we also record

$$\mu \leftarrow \max\{\|\mathbf{A}\Pi(:, j)\|_2^2 : j > s + t, \|\mathbf{A}\Pi(:, j)\|_2^2 < \max_{s < j \leq s+t} \gamma(j)\},$$

which will represent the maximum untracked column norm at the next cycle<sup>6</sup>. The columns associated with  $\mathbf{u}$  are permuted to positions  $(s+t+1):(s+t+r)$  (where  $r = \text{length}(\mathbf{u})$ ) and orthogonalized against the skeleton. We record their new residual norms in  $\gamma$  and we set  $t \leftarrow t + r$ , thus completing the expansion of the “tracked” set.

Algorithm 3.4 summarizes the “expand” step, where  $\mathbf{j}, \beta \leftarrow \text{Threshold}(\mathbf{x}, i, \alpha)$  returns a vector  $\mathbf{j}$  containing all indices  $j \geq i$  such that  $\mathbf{x}(j) \geq \alpha$ , along with the value  $\beta = \max_{j \geq i, j \notin \mathbf{j}} \mathbf{x}(j)$ . For the other functions used in this pseudocode, refer to subsections 3.2 and 3.3.

**3.5. Full Algorithm.** For completeness, we provide full pseudocode for CCEQR in Algorithm 3.5. Note that Algorithm 3.5 allows for a “CSSP only” mode of CCEQR, where only selected columns of  $\mathbf{R}$  are formed, as well as a “full CPQR” version where all Householder reflections are applied to the untracked set to produce all of  $\mathbf{R}$ . This is controlled by the “if-then” block starting at line (12).

We have claimed that CCEQR computes an equivalent column permutation to the Golub-Businger algorithm. We end this section with a formal statement and proof of this claim.

**THEOREM 3.2.** *Let  $\mathbf{p} \in [n]^k$  be the permutation vector returned by Algorithm 3.5. This permutation is equivalent to the one computed by Algorithm 2.1, in the sense that there is a unitary  $\mathbf{Q}$  such that  $\mathbf{Q}^* \mathbf{A}(:, \mathbf{p})$  is in GB( $k$ ) form.*

*Proof.* The proof is inductive. Let  $\mathbf{Q}^{(t)}$  and  $\mathbf{\Pi}^{(t)}$  be the global column permutation and unitary factor at the end of the  $t^{\text{th}}$  cycle of Algorithm 3.5, with  $\mathbf{Q}^{(0)} = \mathbf{I}_{m \times m}$

---

<sup>5</sup>In the rare event that no untracked columns meet the norm threshold, we lower it to  $0.9 \max_{s < j \leq s+t}$  to ensure that the tracked set expands.

<sup>6</sup>This is needed in line (2) of the “commit” step (Algorithm 3.3); see also Lemma 3.1.

---

**Algorithm 3.4** CCEQR: SUBROUTINE “EXPAND”

---

```
1: inputs:  $s, t, M, \gamma, \mathbf{T}, \mathbf{V}, \mathbf{R}$ .

2:  $\mathbf{u}, \mu \leftarrow \text{Threshold}(\gamma, s + t + 1, M)$ .
3:  $r \leftarrow \text{length}(\mathbf{u})$ .
4: if  $r = 0$  then
5:    $\mathbf{u}, \mu \leftarrow \text{Threshold}(\gamma, s + t + 1, 0.9\mu)$ 
6:    $r \leftarrow \text{length}(\mathbf{u})$ .
7: end if

8:  $\mathbf{R} \leftarrow \text{PermuteColumns}(\mathbf{R}, \mathbf{u}, (s + t + 1):(s + t + r), 1:r)$ .
9:  $\gamma \leftarrow \text{PermuteEntries}(\gamma, \mathbf{u}, (s + t + 1):(s + t + r), 1:r)$ .
10:  $\mathbf{p} \leftarrow \text{PermuteEntries}(\mathbf{p}, \mathbf{u}, (s + t + 1):(s + t + r), 1:r)$ .
11:  $\mathbf{R} \leftarrow \text{ApplyQt}(\mathbf{R}, \mathbf{T}, \mathbf{V}, 1:m, (s + t + 1):(s + t + r))$ .

12: for  $j = (s + t + 1):(s + t + r)$  do
13:    $\gamma(j) \leftarrow \gamma(j) - \|\mathbf{R}(1:s, j)\|_2^2$ .
14: end for

15:  $t \leftarrow t + r$ .
```

---

and  $\mathbf{\Pi}^{(0)} = \mathbf{I}_{n \times n}$ . Then  $(\mathbf{Q}^{(0)})^* \mathbf{A} \mathbf{\Pi}^{(0)}$  has GB( $s_0$ ) form with  $s_0 = 0$ . Suppose that  $(\mathbf{Q}^{(t-1)})^* \mathbf{A} \mathbf{\Pi}^{(t-1)}$  has GB( $s_{t-1}$ ) form for some  $t \geq 1$ . The  $t^{\text{th}}$  cycle transforms  $\mathbf{Q}^{(t-1)} \mapsto \mathbf{Q}^{(t)}$  and  $\mathbf{\Pi}^{(t-1)} \mapsto \mathbf{\Pi}^{(t)}$  as described in [Lemma 3.1](#), and the conclusion of that lemma is that  $(\mathbf{Q}^{(t)})^* \mathbf{A} \mathbf{\Pi}^{(t)}$  has GB( $s_{t-1} + c$ ) form for some  $c \in [1, k - s_{t-1}]$ . For some  $T \leq k$  we will therefore have  $s_T = k$ , at which point the algorithm terminates. Hence, the theorem holds with  $\mathbf{Q} = \mathbf{Q}^{(T)}$  and  $\mathbf{A}(:, \mathbf{p}) = \mathbf{A} \mathbf{\Pi}^{(T)}$ .  $\square$

**4. Experiments.** We now present experiments comparing the performance of CCEQR ([Algorithm 3.5](#)) and GEQP3 (the implementation of [Algorithm 2.1](#) in the OpenBLAS LAPACK library). We have selected our test cases to illustrate that the comparison between these two algorithms is strongly affected by the structural properties of the matrix being factorized. [Subsections 4.1](#) and [4.2](#) demonstrate examples from scientific applications where CCEQR outperforms GEQP3 by as much as an order of magnitude. [Subsection 4.3](#) will show that on random unstructured problems, CCEQR and GEQP3 perform more-or-less the same. Finally, [subsection 4.4](#) will demonstrate an “adversarial” problem specifically designed to make CCEQR slower than GEQP3.

Except where stated otherwise, all numerical experiments were performed on a MacBook Air with an M2 chip and 8GB memory, using Julia with OpenBLAS.

**4.1. Spectral Demixing.** Our first test case involves matrices generated as part of a spectral demixing computation. In this setting we consider data points  $\{x_1, \dots, x_n\} \subseteq \mathcal{X}$  drawn i.i.d. from an  $m$ -component mixture model  $\mathcal{P}$ , given by

$$\mathcal{P} = \sum_{i=1}^m \beta_i \mathcal{P}_i, \quad \beta_1, \dots, \beta_m \geq 0, \quad \sum_{i=1}^m \beta_i = 1,$$

where  $\mathcal{P}_1, \dots, \mathcal{P}_m$  are probability measures. We seek to label each point according to which component it was drawn from using spectral clustering [\[37\]](#). To that end,

---

**Algorithm 3.5** COLLECT-COMMIT-EXPAND QR (CCEQR)
 

---

```

1: inputs:  $\mathbf{A} \in \mathbb{C}^{m \times n}$ ,  $k \leq \min\{m, n\}$ ,  $\rho \in (0, 1)$ , and  $\text{FULL} \in \{\text{TRUE}, \text{FALSE}\}$ .

2:  $s, t, \mu, \gamma, \mathbf{p}, \mathbf{V}, \mathbf{T}, \mathbf{R} \leftarrow \text{Initialize}(\mathbf{A}, k)$ .    # see Algorithm 3.1

3: while  $s < k$  do
4:    $\delta, \hat{\tau}, \hat{\mathbf{V}}, \hat{\mathbf{R}} \leftarrow \text{Collect}(\rho, s, t, \gamma, \mathbf{p}, \mathbf{R})$ .    # see Algorithm 3.2
5:    $M \leftarrow \text{Commit}(\delta, \mu, s, t, \gamma, \hat{\tau}, \hat{\mathbf{V}}, \mathbf{T}, \mathbf{V}, \hat{\mathbf{R}}, \mathbf{R})$ .    # see Algorithm 3.3

6:   if  $s < k$  then
7:      $\text{Expand}(s, t, M, \gamma, \mathbf{T}, \mathbf{V}, \mathbf{R})$ .    # see Algorithm 3.4
8:   else
9:     goto line (15).
10:  end if
11: end while

12: if  $\text{FULL} = \text{TRUE}$  then
13:    $\text{ApplyQt}(\mathbf{R}, \mathbf{T}, \mathbf{V}, 1:m, (s+t+1):n)$ .
14: end if

15: return  $\mathbf{p}$ .

```

---

the CPQR factorization to be computed is

$$(4.1) \quad \mathbf{W}_m^T \mathbf{\Pi} = \mathbf{QR},$$

where the columns of  $\mathbf{W}_m$  are the leading  $m$  eigenvectors of the the normalized kernel evaluation matrix  $\mathbf{K}(i, j) = (d_i d_j)^{-1/2} \mathcal{K}(x_i, x_j)$ , with  $\mathcal{K}$  being a positive definite kernel on  $\mathcal{X}$  and  $d_i = \sum_{r=1}^n \mathcal{K}(x_i, x_r)$ . Under suitable conditions on mixture component separation, the leading  $m$ -dimensional eigenspace of  $\mathbf{K}$  approximates  $\mathcal{V} := \text{span}\{\mathbf{v}_1, \dots, \mathbf{v}_m\}$ , where  $\mathbf{v}_i(j)$  is a kernelized measure of likelihood of  $x_j$  under  $\mathcal{P}_i$  [33]. Damle, Minden, and Ying [10] demonstrated that points can be labeled by orthogonalizing  $\mathbf{W}_m^T \mathbf{\Pi}(:, 1:m)$  in (4.1) via a polar decomposition, producing a unitary  $\mathbf{U} \in \mathbb{R}^{m \times m}$  that reveals label likelihoods through the relation  $\mathbf{W}_m \mathbf{U} \approx [\mathbf{v}_1 \cdots \mathbf{v}_m]$ .

Our experiments use  $\mathcal{X} = \mathbb{R}^{20}$ , and points are drawn from an  $m = 20$  component Gaussian mixture model with

$$\mathcal{P}_i = \mathcal{N}(\ell \mathbf{e}_i, \mathbf{I}), \quad \beta_i = 1, \quad i = 1, \dots, m,$$

where  $\mathbf{e}_i$  is the  $i^{\text{th}}$  elementary unit vector and  $\ell$  controls the cluster separation scale. We use  $\mathcal{K}(x, y) = \exp(-\frac{1}{2\sigma^2} \|x - y\|_2^2)$  for the kernel, with kernel variance  $\sigma^2 = 5$ . At the scale of this experiment, working directly with  $\mathbf{K}$  is not computationally feasible. We therefore approximate  $\mathbf{W}_m$  by compressing  $\mathbf{K}$  through a pivoted partial Cholesky factorization with significant oversampling, and then directly computing a singular value decomposition of this low-rank approximation. While techniques for handling  $\mathbf{K}$  are not the focus of this paper, matrix-free kernel manipulation methods such as the fast Gauss transform [21] would also be appropriate in this setting.

Figure 4.1 compares the runtimes of CCEQR and GEQP3 over 100 independent trials. For this experiment we varied the cluster separation lengthscale  $\ell$ , as well as

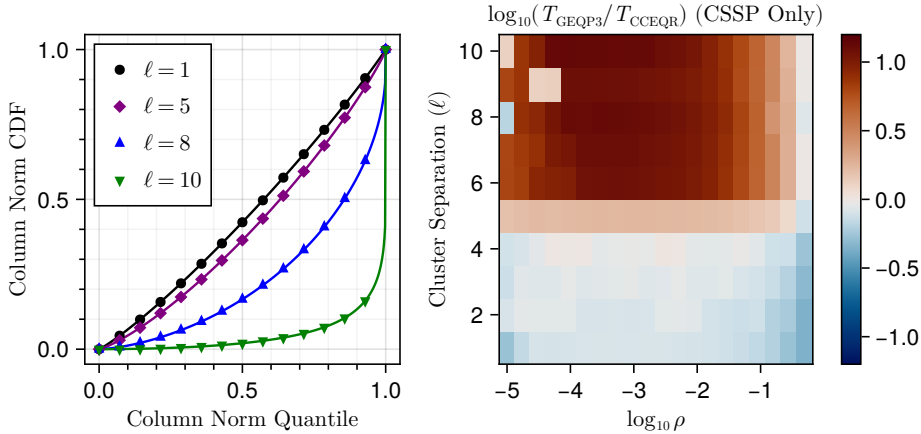


Fig. 4.1: Left-panel: cumulative distribution of column norm mass in  $\mathbf{W}_m^T$  as a function of column norm quantile, versus cluster separation scale  $\ell$ . Right panel: median runtime ratios for CCEQR and GEQP3 on  $m \times n$  matrices generated from spectral demixing with  $m = 20$  components and  $n = 400,000$  data points, across increasing values of  $\rho$  and increasing cluster separation, over 100 trials. Warm colors indicate that CCEQR is faster, and cool colors indicate that GEQP3 is faster. Plotted values range from 0.41 to 15.49. Note that CCEQR was used only to select columns, and the full  $\mathbf{R}$  matrix was not computed.

the parameter  $\rho$  that controls the size of the candidate column block in CCEQR (cf. [subsection 3.2](#)). Increasing  $\ell$  means that a larger number of points will be far from the center of any Gaussian component, corresponding to a larger number of small-norm columns in  $\mathbf{V}_m^T$ . This is shown in the left-hand panel of [Figure 4.1](#) which, for several values of  $\ell$ , plots the percentage of column-norm mass contained at or below a given quantile of the column-norm distribution. Heuristically, we expect CCEQR to run faster than GEQP3 on large problems where the column norm mass is concentrated in a small set of indices (i.e., in the uppermost quantiles). For problems of this sort, the norm-sorting strategy in CCEQR’s “collect” step is more likely to find all necessary skeleton columns early on, which minimizes the amount of work that must be dedicated to Householder reflections. Indeed, [Figure 4.1](#) shows that increasing  $\ell$  leads to a roughly 10x for speedup for CCEQR over GEQP3.

Also apparent in [Figure 4.1](#) are isolated “islands” of longer CCEQR runtimes, visible in the upper-left of the right panel. These correspond to a relatively rare scenario wherein, at some cycle in CCEQR, the entire tracked set lies almost entirely in the subspace spanned by the newly committed skeleton columns. In this situation, orthogonalizing against the new skeleton columns will dramatically reduce residual norms in the tracked set, meaning the threshold  $M$  computed in the “commit” step ([Algorithm 3.3](#)) will be quite small. The “expand” step ([Algorithm 3.4](#)), which adds new tracked columns according to whether or not their norms exceed this threshold, will then make a very large number of columns tracked. The burden of applying Householder reflections to this much larger tracked set greatly slows down future cycles, creating the observed increase in runtimes. In our experience this behavior



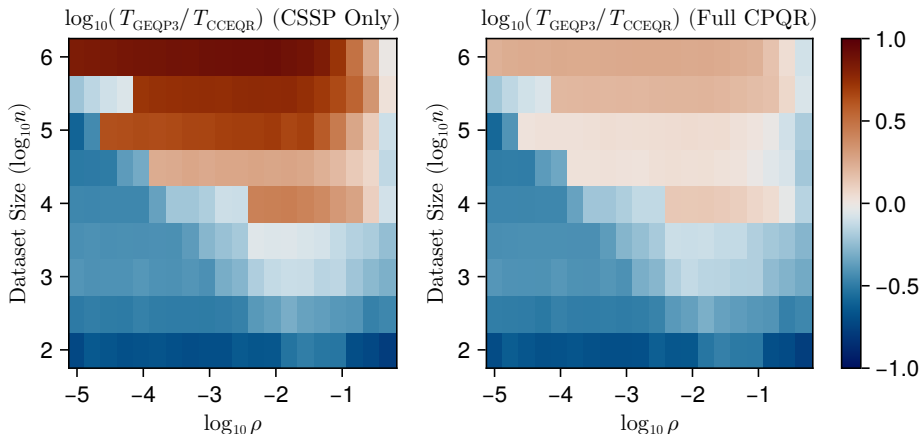


Fig. 4.2: The same experiment as Figure 4.1 with  $\ell = 6$  fixed and  $n$  increasing, with and without full computation of  $\mathbf{R}$  in CCEQR (note that  $\mathbf{R}$  is not needed for the clustering application). Hot colors indicate CCEQR performing faster than GEQP3, while cold colors indicate GEQP3 performing faster. Left panel: plotted values range from 0.18 to 8.31. Right panel: values range from 0.18 to 1.80.

is more likely to occur when  $\rho$  is excessively small, as this produces a small initial tracked set which can be more easily captured in the span of a few skeleton columns.

Figure 4.2 shows an identical experiment to Figure 4.1, except that cluster separation is fixed at  $\ell = 6$  and the dataset size is increased over several orders of magnitude. We note that the extra overhead of CCEQR’s more complex control flow means it is slower than GEQP3 for problems with relatively few columns. For matrices in this experiment with  $10^4$  columns or more, CCEQR is generally faster. This experiment also demonstrates that CCEQR performs best when  $\rho$  is neither too large nor too small. Setting  $\rho$  too large means CCEQR must deal with excessively large candidate blocks at each cycle. On the other hand, setting  $\rho$  to small means that the maximum over tracked residual norms in line (8) of the “commit” step (cf. Algorithm 3.3) is taken over a much smaller set. Because this maximum is used select new tracked columns, (cf. Algorithm 3.4), taking the maximum over too small a set may lead to an unnecessarily large expansion of the tracked set, forcing the algorithm to devote more work to Householder reflections at future cycles. We are pleased to see that for each problem size, the range of “good” choices for  $\rho$  is fairly broad.

**4.2. Density Functional Theory.** A fundamental task in computational chemistry is to compute the ground-state electronic energy of a molecular system, which for a system of  $m$  electrons involves minimizing an energy functional of an  $m$ -particle wavefunction. Density functional theory (DFT) approximates the  $m$ -body ground-state wavefunction in terms of  $m$  single-particle wavefunctions that correspond to the solution of a nonlinear eigenvalue problem [27]. It is computationally advantageous to find a so-called “localized Wannier basis” for the subspace spanned by these wavefunctions, i.e., a basis consisting of vectors whose support is concentrated on a small region of space. Such a basis exists under mild physical assumptions on the electronic system [2]. Damle, Lin, and Ying [9] show how to find a localized Wannier basis by

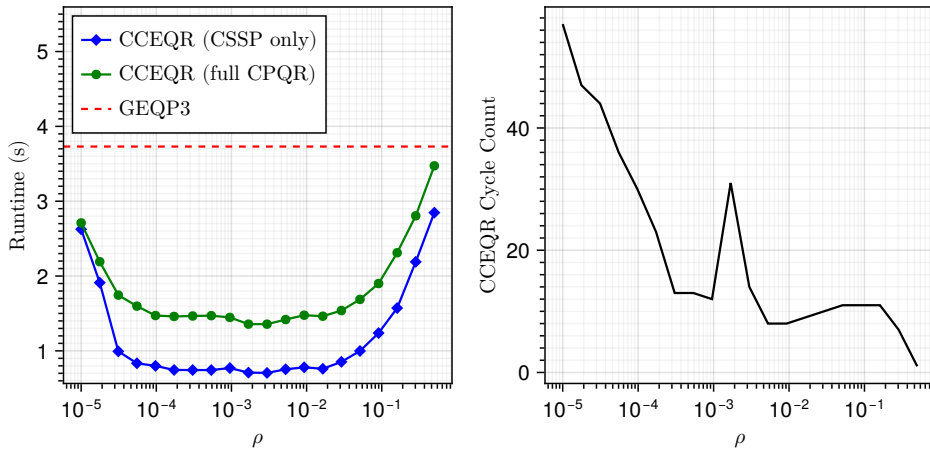


Fig. 4.3: Left: median runtimes for CCEQR and GEQP3 over 10 trials on electronic wavefunctions for alkane with  $m = 110$  and  $n = 820,125$ , selecting  $k = m$  columns, with and without a full Householder reflection at the end of CCEQR. Runtime ratios for GEQP3 over CCEQR range from 1.31 to 5.97 (CSSP only) and from 1.20 to 2.88 (full CPQR); note that the full CPQR is not needed in this application. Right: cycle counts for CCEQR.

means of a CPQR factorization

$$(4.2) \quad \Psi^T \Pi = \mathbf{QR},$$

where  $\Psi \in \mathbb{C}^{n \times m}$  is the matrix of single-particle wavefunctions discretized onto a grid of size  $n$ .

Figure 4.3 compares the runtimes of GEQP3 and CCEQR for computing the column permutation in (4.2), where  $\Psi$  was generated from an alkane molecule with  $m = 110$  and  $n = 820,125$ . For a broad range of values for  $\rho$ , both versions of CCEQR (with and without the final Householder reflection to produce all columns of  $\mathbf{R}$ ) perform significantly faster than GEQP3. Notably, this difference persists even when CCEQR takes many cycles to complete the permutation, indicating that the overhead of the “expand” step is not significant. Refer to subsection 4.1 for a more expansive discussion of how  $\rho$  affects runtime.

Figure 4.4 repeats this experiment for  $\Psi$  generated from a water molecule with  $m = 256$  and  $n = 1,953,125$ . Due to the extreme size of this problem, this experiment was performed on different computing equipment than the other experiments in this paper, namely a Xeon Platinum 8362 core with 1.5TB memory. Here the performance difference between GEQP3 and CCEQR (without full Householder reflections) is even more pronounced, which should not be surprising given that  $m$  and  $n$  have both more-than-doubled relative to the alkane molecule. A striking feature in this experiment is the large spike in cycle count around  $\rho \approx 3 \times 10^{-3}$ . This disrupts our expectation that, as  $\rho$  increases and the candidate blocks become larger, CCEQR should require fewer cycles to find a complete column basis.

To understand this behavior, consider the state of CCEQR immediately after line (9) in the “collect” step (Algorithm 3.2), where  $b$  candidates have been selected out

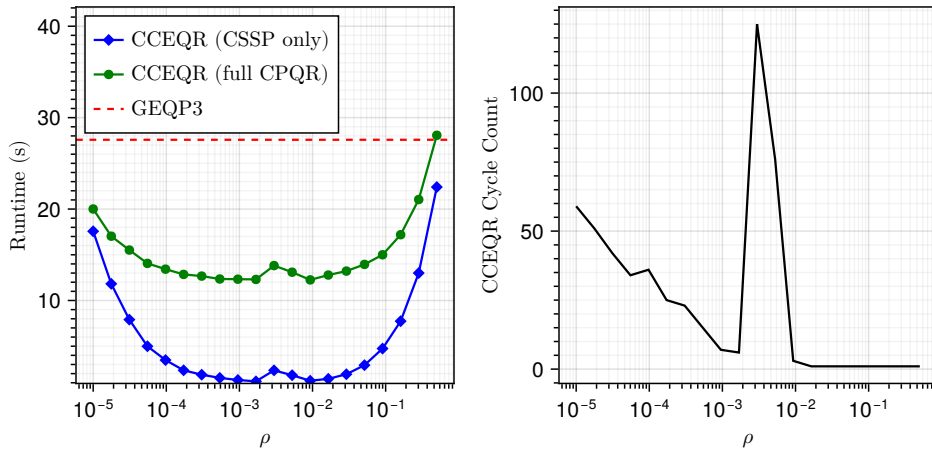


Fig. 4.4: The same experiment as in Figure 4.3, this time using wavefunctions from a water molecule with  $m = 256$  and  $n = 1,953,125$ . See the main text for a discussion of the cycle count spike around  $\rho \approx 3 \times 10^{-3}$ . Runtime ratios for GEQP3 over CCEQR range from 1.26 to 23.81 (CSSP only) and from 1.01 to 2.46 (full CPQR). Note, as before, that the full CPQR is not necessary in this application.

of  $t$  tracked columns. The cycle-count spike in Figure 4.4 corresponds to a situation where there is a large cluster of non-candidate  $j$ 's for which  $\gamma(j)$  is very close to  $\gamma(s+1)$  (where  $s+1$  is the index of the largest-residual candidate column). This can occur at the first cycle if the column norm distribution of the input matrix is near-uniform, and it can also occur more unpredictably at intermediate cycles if the residual matrix happens to acquire a near-uniform norm distribution.

In these cases, CCEQR is unlikely to commit any candidates into the skeleton *except* for the one with largest residual. Indeed, the criterion for accepting a new skeleton column is that its squared-norm orthogonal to the skeleton exceeds the maximum of  $\gamma(j)$  over non-candidates; see equation (3.3) and subsections 3.2 and 3.3. In the situation described, given that the largest-residual candidate barely exceeds this maximum, orthogonalizing the remaining candidates against it is likely to decrease their residual norms below the required threshold. If a very large number of non-candidates are close to this maximum, then unless they are mostly colinear, CCEQR must work through a large number of cycles which each commit only a single column into the skeleton. Once enough of these cycles have taken place to sufficiently reduce residual norms in the cluster of large non-candidates, the algorithm can resume committing multiple columns at a time.

Notably, even when CCEQR encounters an “obstacle” of this sort, Figure 4.4 indicates that the overhead of excessive cycling does not significantly impact its runtime. This is not surprising, for if only a single candidate is committed then finishing the cycle requires only applying a *single* Householder reflector to the tracked set.

**4.3. Gaussian Random Matrices.** Column subset selection problems do not always involve matrices whose column norm distribution is favorable to CCEQR. In light of this, Figure 4.5 compares CCEQR and GEQP3 on completely unstructured

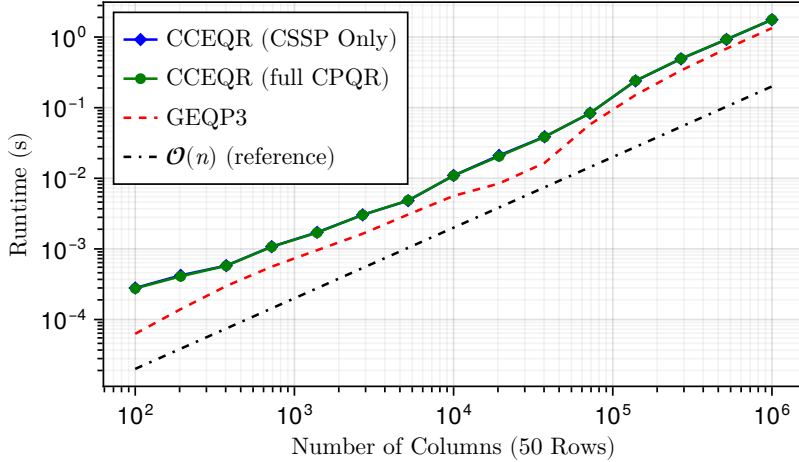


Fig. 4.5: Median runtimes for CCEQR and GEQP3 over 10 trials on test matrices with i.i.d. standard Gaussian entries.

matrices whose entries are i.i.d. standard Gaussians. The results show, primarily, that CCEQR performs nearly the same (albeit slower) than GEQP3 on large unstructured problems. Importantly, CCEQR exhibits  $\mathcal{O}(n)$  runtime scaling for a fixed number of rows, just as GEQP3 does. Note that the runtime differences between CCEQR with and without full computation of  $\mathbf{R}$  are not large enough to be visible on this graph. This is because for unstructured problems of this sort, CCEQR must bring nearly every column of the input matrix into the tracked set. In this case, the extra reflections needed to produce  $\mathbf{R}$  in full cost almost no extra work, since they are only applied to untracked columns at the end of the algorithm.

**4.4. Adversarial Hadamard Matrix.** Our final example is constructed “adversarially” to make CCEQR slower than GEQP3. This involves a matrix  $\mathbf{H}$  consisting of the first  $2^k$  rows from a  $2^r \times 2^r$  diadic Hadamard matrix. Such a matrix has two important properties:

1. all of its columns have equal norm, and
2. its columns can be partitioned into  $2^k$  mutually orthogonal subsets of size  $2^{r-k}$ . Columns within a subset are all colinear.

We have ordered the columns of  $\mathbf{H}$  so that every such subset appears in a contiguous block. To avoid issues related to column norm ties and floating point errors, we have also scaled the  $j^{\text{th}}$  column of  $\mathbf{H}$  by  $1 + 1000(n - j + 1)\eta$  for  $j = 1, \dots, 2^r$ , where  $\eta = 2^{-52}$  is the machine epsilon.

This matrix is “adversarial” for CCEQR in the sense that, at any given cycle, there is an exceedingly large cluster of non-candidate columns whose residual squared norm almost matches that of the largest candidate column. Each cycle is therefore only able to commit a single column into the skeleton, for reasons discussed extensively in [subsection 4.2](#). Our reordering of the columns into colinear blocks is meant to accentuate this behavior, since at every cycle, the orthogonalization step will disqualify remaining candidates in this block from being committed. Furthermore, because all column norms are essentially equal, CCEQR will need to bring every column into

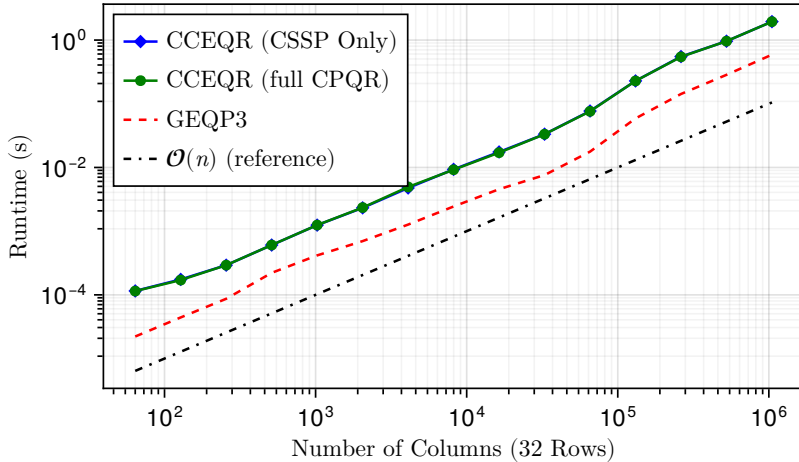


Fig. 4.6: Median runtimes of CCEQR and GEQP3 over 10 trials on an “adversarial”  $2^k \times 2^r$  Hadamard matrix, where  $k = 5$  is fixed and  $r$  is increased from 6 to 20.

the tracked set, meaning significant work will be devoted to Householder reflections.

Figure 4.6 shows runtimes of CCEQR and GEQP3 on this class of matrices, where  $k = 5$  is fixed and  $r$  is increased from 6 to 20. As in the random Gaussian test cases (cf. subsection 4.3), both CCEQR and GEQP3 exhibit  $\mathcal{O}(n)$  scaling for a fixed number of rows. Because the entire column set becomes tracked, there is also no perceptible runtime difference between CCEQR with and without full computation of  $\mathbf{R}$ . It is encouraging that even for this “adversarial” example, CCEQR differs from GEQP3 in runtime by less than an order of magnitude. However, in contrast to the random Gaussian test cases, there is a persistent  $\sim 2x$  runtime difference which is not eliminated by increasing the problem size.

**5. Conclusions.** We have demonstrated an efficient CPQR-based column subset selection algorithm called CCEQR. This algorithm differs from existing CPQR-based rapid column selection algorithms in that (1) it is targeted toward matrices with far more columns than rows, (2) it is deterministic, and (3) it provably recovers the same column choice as the Golub Businger algorithm. Our algorithm is specifically designed for matrices whose column norm distribution has rapid decay. Using test matrices coming from applications in spectral clustering and density functional theory, which naturally have rapidly decaying column norms, we have demonstrated that CCEQR can run significantly faster than the LAPACK implementation of the Golub Businger algorithm (GEQP3). Although CCEQR can often outperform GEQP3 on the computation of a full column-pivoted QR factorization, the performance difference is most apparent for problems that only require computing the column permutation. We have also found that for problems whose column norm distribution is uniform, the performance difference between our algorithm and GEQP3 is small.

**6. Acknowledgements.** RA and AD were partially supported by the National Science Foundation award DMS-2146079 and the Department of Energy Office of Science award DE-SC0025453. AD was also partially supported by the SciAI Center,

funded by the Office of Naval Research under Grant Number N00014-23-1-2729.

#### REFERENCES

- [1] R. ARMSTRONG, A. BUZALI, AND A. DAMLE, *Structure-aware analyses and algorithms for interpolative decompositions*, 2023, <https://arxiv.org/abs/2310.09452>.
- [2] M. BENZI, P. BOITO, AND N. RAZOUK, *Decay properties of spectral projectors with applications to electronic structure*, SIAM Review, 55 (2013), pp. 3–64.
- [3] C. BISCHOF AND C. VAN LOAN, *The WY representation for products of Householder matrices*, SIAM Journal on Scientific and Statistical Computing, 8 (1987), pp. s2–s13.
- [4] C. H. BISCHOF, *A parallel QR factorization algorithm with controlled local pivoting*, SIAM Journal on Scientific and Statistical Computing, 12 (1991), pp. 36–57.
- [5] P. BUSINGER AND G. H. GOLUB, *Linear least squares solutions by Householder transformations*, Numerische Mathematik, 7 (1965), pp. 269 – 276.
- [6] S. CHANDRASEKARAN AND I. C. F. IPSEN, *On rank-revealing factorisations*, SIAM Journal on Matrix Analysis and Applications, 15 (1994), pp. 592–622.
- [7] S. CHATURANTABUT AND D. C. SORENSEN, *Nonlinear model reduction via discrete empirical interpolation*, SIAM Journal on Scientific Computing, 32 (2010), pp. 2737–2764.
- [8] A. DAMLE, S. GLAS, A. TOWNSEND, AND A. YU, *How to reveal the rank of a matrix?*, 2024, <https://arxiv.org/abs/2405.04330>.
- [9] A. DAMLE, L. LIN, AND L. YING, *Compressed representation of Kohn-Sham orbitals via selected columns of the density matrix*, J Chem Theory Comput, 14 (2015), pp. 1463–1469.
- [10] A. DAMLE, V. MINDEN, AND L. YING, *Simple, direct and efficient multi-way spectral clustering*, Information and Inference: A Journal of the IMA, 8 (2018), pp. 181–203.
- [11] J. W. DEMMEL, L. GRIGORI, M. GU, AND H. XIANG, *Communication avoiding rank revealing QR factorization with column pivoting*, SIAM Journal on Matrix Analysis and Applications, 36 (2015), pp. 55–89.
- [12] A. DESHPANDE AND L. RADEMACHER, *Efficient volume sampling for row/column subset selection*, in 2010 IEEE 51st Annual Symposium on Foundations of Computer Science, 2010, pp. 329–338.
- [13] A. DESHPANDE, L. RADEMACHER, S. VEMPALA, AND G. WANG, *Matrix approximation and projective clustering via volume sampling*, in Proceedings of the Seventeenth Annual ACM-SIAM Symposium on Discrete Algorithm, SODA '06, USA, 2006, Society for Industrial and Applied Mathematics, p. 1117–1126.
- [14] P. DRINEAS, M. W. MAHONEY, AND S. MUTHUKRISHNAN, *Relative-error CUR matrix decompositions*, SIAM Journal on Matrix Analysis and Applications, 30 (2008), pp. 844–38.
- [15] Z. DRMAČ AND Z. BUJANOVIĆ, *On the failure of rank-revealing QR factorization software – a case study*, ACM Trans. Math. Softw., 35 (2008).
- [16] Z. DRMAČ AND S. GUGERCIN, *A new selection operator for the discrete empirical interpolation method—improved a priori error bound and extensions*, SIAM Journal on Scientific Computing, 38 (2016), pp. A631–A648.
- [17] J. A. DUERSCH AND M. GU, *Randomized QR with column pivoting*, SIAM Journal on Scientific Computing, 39 (2017), p. C263–C291.
- [18] A. FRIEZE, R. KANNAN, AND S. VEMPALA, *Fast Monte-Carlo algorithms for finding low-rank approximations*, J. ACM, 51 (2004), p. 1025–1041.
- [19] G. H. GOLUB, V. KLEMA, AND G. STEWART, *Rank degeneracy and least squares problems*, Tech. Report STAN-CS-76-559, Stanford University, 1976.
- [20] G. H. GOLUB AND C. F. V. LOAN, *Matrix Computations*, Johns Hopkins University Press, fourth ed., 2013.
- [21] L. GREENGARD AND J. STRAIN, *The fast Gauss transform*, SIAM Journal on Scientific and Statistical Computing, 12 (1991), pp. 79–94.
- [22] M. GU AND S. C. EISENSTAT, *Efficient algorithms for computing a strong rank-revealing QR factorization*, SIAM Journal on Scientific Computing, 17 (1996), pp. 848–869.
- [23] N. HALKO, P. G. MARTINSSON, AND J. A. TROPP, *Finding structure with randomness: Probabilistic algorithms for constructing approximate matrix decompositions*, SIAM Review, 53 (2011), pp. 217–288.
- [24] Y. HONG AND C.-T. PAN, *Rank-revealing QR factorizations and the singular value decomposition*, Mathematics of Computation, 58 (1992), pp. 213 – 232.
- [25] W. KAHAN, *Numerical linear algebra*, Canad. Math. Bull., 9 (1966), pp. 757–801.
- [26] E. LIBERTY, F. WOOLFE, P.-G. MARTINSSON, V. ROKHLIN, AND M. TYGERT, *Randomized algorithms for the low-rank approximation of matrices*, Proceedings of the National Academy

- of Sciences, 104 (2007), pp. 20167–20172.
- [27] L. LIN AND J. LU, *A Mathematical Introduction to Electronic Structure Theory*, Society for Industrial and Applied Mathematics, Philadelphia, PA, 2019.
- [28] M. W. MAHONEY AND P. DRINEAS, *CUR matrix decompositions for improved data analysis*, Proceedings of the National Academy of Sciences, 106 (2009), pp. 697–702.
- [29] P.-G. MARTINSSON, G. QUINTANA ORTÍ, N. HEAVNER, AND R. VAN DE GEIJN, *Householder QR factorization with randomization for column pivoting (HQRRP)*, SIAM Journal on Scientific Computing, 39 (2017), pp. C96–C115.
- [30] R. MURRAY, J. DEMMEL, M. W. MAHONEY, N. B. ERICHSON, M. MELNICHENKO, O. A. MALIK, L. GRIGORI, P. LUSZCZEK, M. DEREZIŃSKI, M. E. LOPES, T. LIANG, H. LUO, AND J. DONGARRA, *Randomized numerical linear algebra : A perspective on the field with an eye to software*, 2023, <https://arxiv.org/abs/2302.11474>, <https://arxiv.org/abs/2302.11474>.
- [31] G. QUINTANA-ORTÍ, X. SUN, AND C. H. BISCHOF, *A BLAS-3 version of the QR factorization with column pivoting*, SIAM Journal on Scientific Computing, 19 (1998), pp. 1486–1494.
- [32] A. K. SAIBABA, *Randomized discrete empirical interpolation method for nonlinear model reduction*, SIAM Journal on Scientific Computing, 42 (2020), pp. A1582–A1608.
- [33] G. SCHIEBINGER, M. J. WAINWRIGHT, AND B. YU, *The geometry of kernelized spectral clustering*, The Annals of Statistics, 43 (2015), pp. 819 – 846.
- [34] R. SCHREIBER AND C. VAN LOAN, *A storage-efficient WY representation for products of Householder transformations*, SIAM Journal on Scientific and Statistical Computing, 10 (1989).
- [35] D. C. SORENSEN AND M. EMBREE, *A DEIM induced CUR factorization*, SIAM Journal on Scientific Computing, 38 (2016), pp. A1454–A1482.
- [36] R. VERSHYNIN, *Four lectures on probabilistic methods for data science*, in The Mathematics of Data, American Mathematical Society, 2018, pp. 231–271.
- [37] U. VON LUXBURG, *A tutorial on spectral clustering*, Statistics and Computing, 17 (2007), pp. 395–416.
- [38] F. WOOLFE, E. LIBERTY, V. ROKHLIN, AND M. TYGERT, *A fast randomized algorithm for the approximation of matrices*, Applied and Computational Harmonic Analysis, 25 (2008), pp. 335–366.
- [39] A. ÇIVRIL AND M. MAGDON-ISMAIL, *On selecting a maximum volume sub-matrix of a matrix and related problems*, Theoretical Computer Science, 410 (2009), pp. 4801–4811.

**Appendix A. Proof of Lemma 3.1.** Let  $\mathbf{Q}, \mathbf{\Pi}$  be the CPQR factors at the beginning of a given cycle of CCEQR, and define  $\mathbf{R}^{(0)} = \mathbf{Q}^* \mathbf{A} \mathbf{\Pi}$ , a matrix in GB( $s$ ) form. Let  $\hat{\mathbf{Q}}, \hat{\mathbf{\Pi}}$ , and  $c$  be defined as in Lemma 3.1. For the purposes of this proof, the important properties of  $\hat{\mathbf{Q}}$  and  $\hat{\mathbf{\Pi}}$  are as follows.

- Columns  $(s+1) : (s+t)$  of  $\mathbf{R}^{(0)}$  are arranged by  $\hat{\mathbf{\Pi}}$  into an order determined using GEQP3 at line (6) of the “collect” step (Algorithm 3.2), and all other columns are left in place.
- Rows  $(s+1) : m$  of  $\mathbf{R}^{(0)}$  are transformed by  $\hat{\mathbf{Q}}$  using the first  $c$  Householder reflectors from GEQP3, and all other rows are left unchanged.

Our goal in this section is to show that  $\mathbf{R}^{(1)} := (\hat{\mathbf{Q}}\hat{\mathbf{Q}})^* \mathbf{A} (\hat{\mathbf{\Pi}}\hat{\mathbf{\Pi}}) = \hat{\mathbf{Q}}^* \mathbf{R}^{(0)} \hat{\mathbf{\Pi}}$  has GB( $s+c$ ) form. Before proceeding, let us check that the maximum defining  $c$  in (3.3) is over a nonempty set, so that  $c \geq 1$  is well-defined. In the notation of subsection 3.2, let  $\mathbf{B} := \mathbf{R}^{(0)}((s+1) : m, s + \sigma(1 : b))$  be the block of residual candidate columns, such that

$$\hat{\mathbf{p}}, \hat{\boldsymbol{\tau}}, \hat{\mathbf{V}}, \hat{\mathbf{R}} \leftarrow \text{GEQP3}(\mathbf{B})$$

is the factorization performed at line (6) of the “collect” step (Algorithm 3.2). Recall that  $c = \max \mathcal{I}$ , where

$$\mathcal{I} = \{i \geq 1 : |\hat{\mathbf{R}}(i, i)|^2 \geq \delta \vee \mu\},$$

$$\delta = \max_{s+b < j \leq s+t} \|\mathbf{R}^{(0)} \hat{\mathbf{\Pi}}((s+1) : m, j)\|_2^2, \quad \mu = \max_{s+t < j \leq n} \|\mathbf{A} \mathbf{\Pi}(:, j)\|_2^2.$$

Because the candidate block of the  $b$  tracked columns with greatest residual norm (cf.

subsection 3.2), we know that

$$|\widehat{\mathbf{R}}(1, 1)|^2 = \max_{1 \leq j \leq b} \|\mathbf{B}(:, j)\|_2^2 = \max_{s < j \leq s+t} \|\mathbf{R}^{(0)} \widehat{\mathbf{\Pi}}((s+1) : m, j)\|_2^2 \geq \delta.$$

Also, letting  $\gamma$  be the vector of residual column norms at the beginning of the given cycle, (3.1) shows that

$$|\widehat{\mathbf{R}}(1, 1)|^2 = \max_{s < j \leq s+t} \gamma(j) \geq \max_{s+t < j \leq n} \|\mathbf{A} \mathbf{\Pi}(:, j)\|_2^2 = \mu.$$

We now see that  $1 \in \mathcal{I}$ , so the maximum defining  $c$  is well-defined.

Turning now to the main claim of Lemma 3.1, the first requirement of  $\text{GB}(s+c)$  form is that  $\mathbf{R}^{(1)}(:, 1:(s+c))$  is upper-triangular. This follows from the construction of  $\widehat{\mathbf{Q}}$  and  $\widehat{\mathbf{\Pi}}$  with GEQP3. The second requirement is that for all indices  $1 \leq i \leq s+c$  and  $i \leq j \leq n$ ,

$$(A.1) \quad |\mathbf{R}^{(1)}(i, i)| \geq \|\mathbf{R}^{(1)}(i : m, j)\|_2.$$

We prove this by cases.

1. For  $i \leq s$  we rely on the fact that  $\mathbf{R}^{(1)}(i, i) = \mathbf{R}^{(0)}(i, i)$ , and we consider two sub-cases.
  - 1a. If  $j \leq s$  or  $j > s+t$  then  $\|\mathbf{R}^{(1)}(i : m, j)\|_2 = \|\mathbf{R}^{(0)}(i : m, j)\|_2$ , as  $\mathbf{R}^{(1)}(i : m, j)$  differs from  $\mathbf{R}^{(0)}(i : m, j)$  by a rotation in the lower  $m-s$  indices. This means that (A.1) follows from the  $\text{GB}(s)$  form of  $\mathbf{R}^{(0)}$ .
  - 1b. If  $s < j \leq s+t$ , then there is a  $p \in [s+1, s+t]$  determined by  $\widehat{\mathbf{\Pi}}$  such that  $\mathbf{R}^{(1)}(i : m, j)$  and  $\mathbf{R}^{(0)}(i : m, p)$  differ by only a rotation in the lower  $m-s$  indices. Thus  $\|\mathbf{R}^{(1)}(i : m, j)\|_2 = \|\mathbf{R}^{(0)}(i : m, p)\|_2$ , so once again, (A.1) follows from the  $\text{GB}(s)$  form of  $\mathbf{R}^{(0)}$ .
2. For  $s < i \leq s+c$ , we again consider sub-cases based on  $j$ .
  - 2a. If  $j \leq s+b$  then

$$\begin{aligned} \mathbf{R}^{(1)}(i, i) &= \widehat{\mathbf{R}}(i-s, i-s) \\ \mathbf{R}^{(1)}(i : m, j) &= \widehat{\mathbf{R}}((i-s) : (m-s), j-s). \end{aligned}$$

In this case, (A.1) holds because GEQP3 outputs  $\widehat{\mathbf{R}}$  in  $\text{GB}(d)$  form (with  $d = \min\{m-s, b\}$ ).

- 2b. If  $s+b < j \leq s+t$  then, by (3.3) and the  $\text{GB}(d)$  form of  $\widehat{\mathbf{R}}$ ,

$$\begin{aligned} |\mathbf{R}^{(1)}(i, i)|^2 &= |\widehat{\mathbf{R}}(i-s, i-s)|^2 \geq |\widehat{\mathbf{R}}(c, c)|^2 \\ &\geq \delta = \max_{s+b < j' \leq s+t} \|\mathbf{R}^{(0)} \widehat{\mathbf{\Pi}}((s+1) : m, j')\|_2^2 \\ &= \max_{s+b < j' \leq s+t} \|\mathbf{R}^{(1)}((s+1) : m, j')\|_2^2 \\ &\geq \|\mathbf{R}^{(1)}(i : m, j)\|_2^2, \end{aligned}$$

as desired.

- 2c. Finally, if  $s+t < j$  then

$$\begin{aligned} |\mathbf{R}^{(1)}(i, i)|^2 &\geq |\widehat{\mathbf{R}}(c, c)|^2 \geq \mu = \max_{s+t < j' \leq n} \|\mathbf{A} \mathbf{\Pi}(:, j')\|_2^2 \\ &= \max_{s+t < j' \leq n} \|\mathbf{R}^{(1)}(:, j')\|_2^2 \\ &\geq \|\mathbf{R}^{(1)}(i : m, j)\|_2^2, \end{aligned}$$

completing the proof.



**Appendix B. Efficient Updates of Householder Reflectors.** Given  $m \times m$  unitary matrices  $\mathbf{Q}_1 = \mathbf{I} - \mathbf{V}_1 \mathbf{T}_1 \mathbf{V}_1^*$  and  $\widehat{\mathbf{Q}} = \mathbf{I} - \widehat{\mathbf{Q}} \widehat{\mathbf{T}} \widehat{\mathbf{Q}}^*$  in compact WY form, this section addresses the task of forming a compact WY representation of  $\mathbf{Q}_2 := \mathbf{Q}_1 \widehat{\mathbf{Q}}$  using BLAS-3 operations. In the context of CCEQR,  $\mathbf{Q}_1$  represents the unitary factor at the beginning of a given cycle, and  $\widehat{\mathbf{Q}}$  consists of the first  $c$  Householder reflectors computed by GEQP3 in the “collect” stage (Algorithm 3.2). We write

$$\mathbf{V}_1 = [\mathbf{v}_1 \ \cdots \ \mathbf{v}_s], \quad \widehat{\mathbf{V}} = [\mathbf{v}_{s+1} \ \cdots \ \mathbf{v}_{s+c}], \quad \mathbf{V}_2 = [\mathbf{v}_1 \ \cdots \ \mathbf{v}_{s+c}].$$

By construction,  $\mathbf{V}_2$  is upper-triangular with unit diagonal. We have assumed here that  $\widehat{\mathbf{V}}$  is padded with zeros in the first few rows to have conformal dimensions with  $\mathbf{V}_1$ , even though in subsection 3.3,  $\widehat{\mathbf{V}}$  denotes the raw output of GEQP3 without zero padding. Lemma B.1 provides the needed update formulas.

LEMMA B.1. *If  $\mathbf{I} - \mathbf{V}_2 \mathbf{T}_2 \mathbf{V}_2^*$  is the compact WY form for  $\mathbf{Q}_2$ , then*

$$\mathbf{T}_2 = \begin{bmatrix} \mathbf{T}_1 & -\mathbf{T}_1 \mathbf{V}_1^* \widehat{\mathbf{V}} \widehat{\mathbf{T}} \\ \mathbf{0} & \widehat{\mathbf{T}} \end{bmatrix}.$$

*Proof.* Inserting compact WY forms into  $\mathbf{Q}_2 = \mathbf{Q}_1 \widehat{\mathbf{Q}}$ , we have

$$\mathbf{I} - \mathbf{V}_2 \mathbf{T}_2 \mathbf{V}_2^* = \mathbf{I} - \mathbf{V}_1 \mathbf{T}_1 \mathbf{V}_1^* - \widehat{\mathbf{V}} \widehat{\mathbf{T}} \widehat{\mathbf{V}}^* + \mathbf{V}_1 \mathbf{T}_1 \mathbf{V}_1^* \widehat{\mathbf{V}} \widehat{\mathbf{T}} \widehat{\mathbf{V}}^*,$$

and because  $\mathbf{V}_2 = [\mathbf{V}_1 \ \widehat{\mathbf{V}}]$ , this implies that

$$\begin{aligned} \mathbf{V}_2 \mathbf{T}_2 \mathbf{V}_2^* &= \mathbf{V}_1 \mathbf{T}_1 \mathbf{V}_1^* + \widehat{\mathbf{V}} \widehat{\mathbf{T}} \widehat{\mathbf{V}}^* - \mathbf{V}_1 \mathbf{T}_1 \mathbf{V}_1^* \widehat{\mathbf{V}} \widehat{\mathbf{T}} \widehat{\mathbf{V}}^* \\ &= \mathbf{V}_2 \begin{bmatrix} \mathbf{T}_1 & -\mathbf{T}_1 \mathbf{V}_1^* \widehat{\mathbf{V}} \widehat{\mathbf{T}} \\ \mathbf{0} & \widehat{\mathbf{T}} \end{bmatrix} \mathbf{V}_2^*. \end{aligned}$$

Because  $\mathbf{V}_2$  is a lower-triangular  $m \times (s+c)$  matrix with unit diagonal, it has full column rank. We have used here the fact that, in the context of CCEQR,  $s+c \leq k \leq m$ . Therefore, multiplying by  $\mathbf{V}_2^\dagger$  on the left and  $(\mathbf{V}_2^*)^\dagger$  on the right proves the claim.  $\square$